DETERMINATION OF FACTORS TO IMPROVE EFFECTIVENESS OF TRIANGULATION MEMBERS FOR A FORMULA SAE RACE CAR FRAME

By

VIKRAM NAIR

Presented to the Faculty of the Graduate School of

The University of Texas at Arlington in Partial Fulfillment

of the Requirements

for the Degree of

MASTER OF SCEINCE IN MECHANICAL ENGINEERING

THE UNIVERSITY OF TEXAS AT ARLINGTON

MAY 2012

ACKNOWLEDGEMENTS

I would like to acknowledge my family for providing me with all the resources in order to achieve my goal of studying abroad. With their love and support the past couple of years have been life changing and pushed me to fulfill my goals of being a successful engineer.

I would like to thank Dr. Robert Woods for his immense help in guiding me to take on new projects and enhance my knowledge & skills. Without the encouragement provided by him and his tireless enthusiasm to see his students succeed, I would certainly not have reached the level where I am today.

I thank Dr. Lawrence and Dr. Robert Taylor for their support and contribution to the completion of my thesis and also my graduate education. Also I would like to thank all the other professors who mentored me over the years.

My reason for coming to UTA was to join the Formula SAE team and I would like to thank all my fellow team members and associates for helping me to learn so much in such little time. Last but not least I would like to thank my friends at UTA for helping me every step of the way.

April 18, 2012

ABSTRACT

DETERMINATION OF FACTORS TO IMPROVE EFFECTIVENESS OF TRIANGULATION MEMBERS FOR A FORMULA SAE RACE CAR FRAME

Vikram Nair, M.S.

The University of Texas at Arlington, 2012

Supervising Professor: Robert Woods

This thesis suggests which factors have significant effect on the torsional and flexural stiffness of a space frame without contributing excessively to its weight. These factors are used as design variables to display the interaction plots generated by performing a Design of Experiments (DOE) using the Hyperstudy tool in Hyperworks by Altair®. The DOE will also provide a mathematical model which can help predict the responses by varying several factors in the design. The node - element models are created in ANSYS classic and are analyzed for various load cases that are representative of the loads on a formula SAE chassis during operation. The main focus is to maximize stiffness to weight ratio for a simple rectangular space frame while keeping making sure the various stresses acting along the section is under the yield load.

TABLE OF CONTENTS

LIST OF ILLUSTRATIONS

Figure Page

LIST OF TABLES

CHAPTER 1

INTRODUCTION

The design of a frame for vehicular applications depends on various factors in order to be efficient in fulfilling its purpose. Over the years various designs have been implemented which vary from space frames to the recent monocoque design. These concepts are efficient in their own way based on their application and manufacturing techniques available. As described in the book *Racing and Sports Car Chassis Design,* the basic purpose of the race car chassis is to connect all four wheels with a structure which is rigid in bending and torsion (which will neither sag or twist) and also must be capable of supporting all the components and occupants by absorbing loads without deflecting excessively. [1]

The requirements of chassis depend heavily on the type of application it is used for. Various types of chassis designs have their individual strengths and weaknesses. Every type of chassis is a compromise between size, complexity, weight, application and overall cost. There is so ideal method of construction of a vehicle chassis as each of them present a different set of parameters/problems. Given the variation in design and construction, every chassis should be designed to the following basic specification,

1. It should be structurally efficient and must not deform or break over the expected life of the design under normal conditions.
2. It should be able to withstand the suspension loads in order to ensure safe and tunable handling of the vehicle for various types of loads.

3. It should support all the other components of the vehicle such as the engine, battery, etc without affecting the function of the chassis over the expected life of the design.
4. It should protect the driver and other occupants of the vehicle from any sort of external intrusion.

1.1 Types of Frame Designs

The main types of frame design used for a race car application are discussed below,

1.1.1 Twin Tube or Ladder Frame

In the early 60's, this type of frame was commonly used in standard cars. Like the name suggests it has two longitudinal rails interconnected by several lateral and cross braces which makes this type of frame easier to construct. The major drawback of this design is that the lateral loads are less compensated as the longitudinal rails are the main stress members. Hence this type of frame design lacks torsional rigidity. [2]

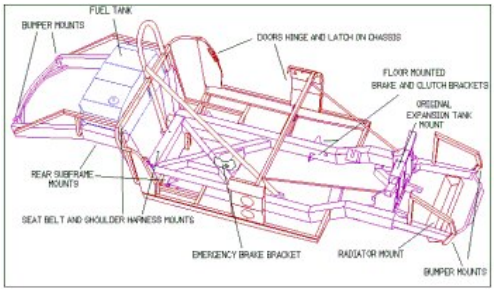

Figure 1.1 Twin Tube or Ladder Frame

1.1.2 Backbone Chassis

The backbone chassis has a simple design which incorporates a strong tubular backbone, usually in a rectangular section, which connects the front and the rear axle and provides mechanical strength. This type of chassis is strong enough for smaller sports cars but

lacks strength for high end ones as it does not provide protection for side impact or offset crash. It is easier to manufacture owing to its simple design and also the most space saving other than a monocoque chassis. [2]

Figure 1.2 Backbone chassis

1.1.3 Tubular Space Frame

The space frame is the most efficient type of chassis which can be built in limited production. The design of the space frame is such that it can take loads in all directions and thus is not only torsionally rigid but also rigid in bending. Further details of this type are described in the next section. [1]

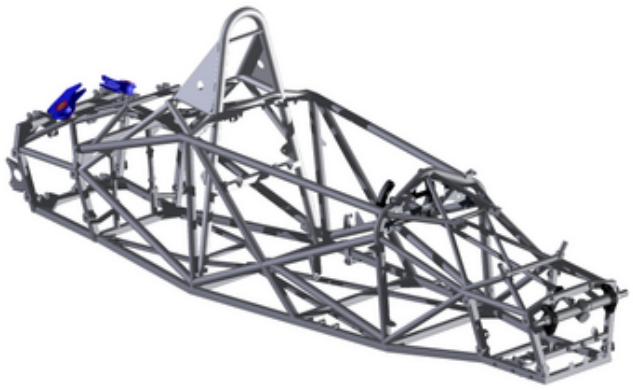

Figure 1.3 Tubular space frame

1.1.4 Monocoque

Monocoque is a one-piece structure which defines the overall shape of the car. While the previous types mentioned above need to build the body around them, the monocoque chassis is already incorporated with the body in a single piece. This design should be stiffer than an equivalent tubular space frame and body for the same weight or lighter for similar stiffness. Monocoque chassis also benefit in crash protection as well as space efficiency. [1, 2]

Figure 1.4 Monocoque

From all the various types of frames mention above, Space frames are the most common type used in the Formula SAE collegiate competition as they are simpler in design and easier to manufacture for a weekend autocross driver. Hence we further look into the concept of space frames and ways to make them torsionally rigid and decrease complexity of manufacturing.

1.2 Space Frames

Space frames in a broader sense are defined as follows,

"A space frame is a structure system assembled of linear elements so arranged that forces are transferred in a three-dimensional manner. In some cases, the constituent element may be two dimensional. Macroscopically a space frame often takes the form of a flat or curved surface." [3]

Space frames are commonly used at the Formula SAE collegiate competition for the following reasons,

1. Simplicity in design and manufacturing
2. The size of various sections of the car can be designed as per the suspension setup and geometry
3. Steel or aluminum tubes placed in a triangulated format can be setup to support the loads from the suspension, engine, driver and aerodynamics of the car.
4. It can easily be inspected for damage and hence easily repaired.

The Formula SAE rules have evolved over the years on tubing size specification used in order to design a space frame. These rules mainly deal with the critical sections of the frame such as the main and front roll hoops and their bracing, the front bulkhead and its bracing and also the side impact structure of the car. The rules also specify fixed templates for the minimum cockpit opening size and also for the driver's feet from the front roll hoop. All the other tubes are selected and laid out based on the suspension pickup points and the placement of the engine and drivetrain. These tubes have to be positioned so as to achieve maximum torsional and bending stiffness without adding excessive weight to the structure.

The frame geometry should be such that the loads act in tensile and compressive manner in the frame members. Also the moment of inertia of the frame should be minimized which will affect the handling of the car during lateral maneuvers and braking. By following these guidelines, a high stiffness to weight ratio can be obtained.

1.2.1 Triangulation of space frames

The effectiveness of a space frame depends on its triangulation. As the size of the frame increase, the space in between also increases which results in a decrease in structural rigidity of the frame. One of the objectives of this thesis is to determine at what size of a given structure is it necessary to add triangulation so as to have a significant effect on the stiffness without excessively adding weight to the structure.

In order to understand the effect of triangulation on a structure, the following 2-D example can be considered. Consider a rectangle supported at its base and a force is applied to one side of the rectangle. The structure tends to bend in the direction of the force quite easily and hence is inefficiently stiff.

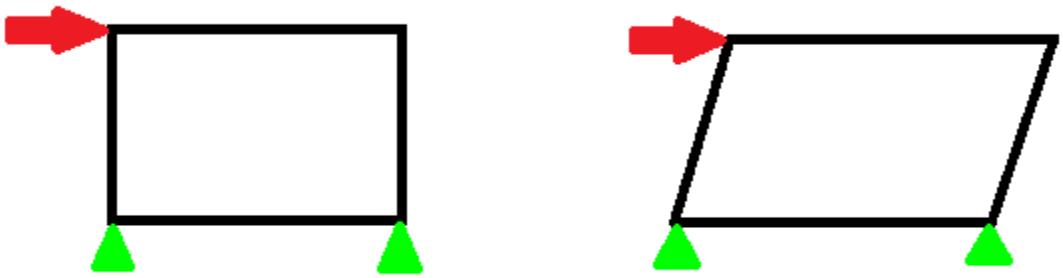

Figure 1.5 Deformation of rectangular structure without triangulation

If we add a diagonal in the orientation shown below, it increases the overall stiffness of the structure. This diagonal member now acts in tension as the forces induced are trying to pull the diagonal from each end. The stiffness of this member acting in tension is higher than the compared to the stiffness of the sides of the rectangular structure in bending.

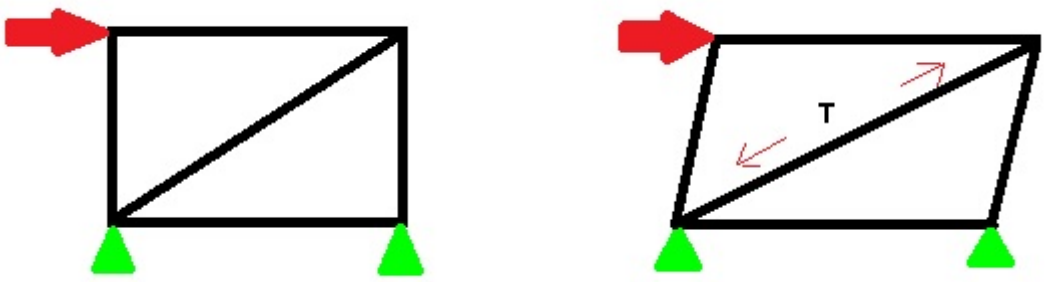

Figure 1.6 Deformation of rectangular structure with triangulation in Tension

By reversing the direction of the diagonal member, the direction of the force changes and thus the member now acts in compression. This orientation of the diagonal members can lead to buckling of the triangulation and hence would need to be further strengthened by adding material. For example, it is far easier to crush an empty can of coke than to pull it apart from end to end. Hence Tubing which is used in tension can be of a lighter gauge than that used in compression. [4]

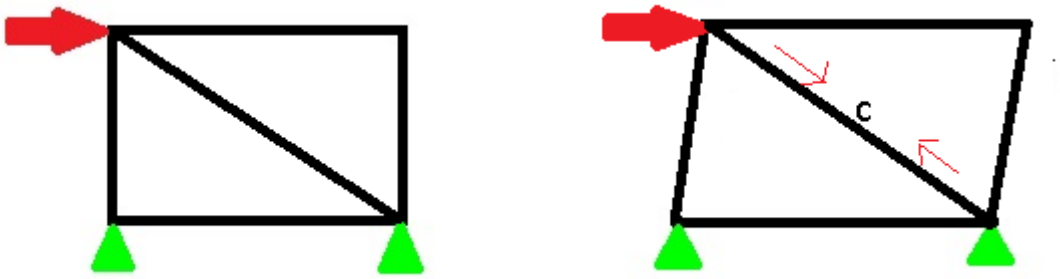

Figure 1.7 Deformation of rectangular structure with triangulation in Compression.

From the example shown above, the same can be applied to three dimensional structures in order to increase its stiffness. The triangulated bays formed by these members in 3-D are called tetrahedrons which are quite stiff in its design. They also help in the formation of nodes on the chassis to aid in the stress distribution under various load cases.

In terms of application of these structures on the chassis, it is quite difficult to get the ideal shape of a tetrahedron as it would make the chassis impractical. For example, the best way to stiffen the suspension bays of a chassis would be to put a diagonal across it but in doing so would obstruct the driver's legs.

1.3 Objective of the thesis

The main objective is to determine the factors that have a significant effect on the stiffness to weight ratio of a rectangular space frame. This analysis will provide data for estimating the interaction between the design variables and the response. From the data, we can approximate a mathematical model to predict the effect of these design variables for a given range of variation. This range is specified by the rules required for the design of a Formula SAE car.

The steps taken to achieve the afore mentioned objective are as follows,

1) Create node-element model in ANSYS APDL of a rectangular section of the frame and apply the required forces and restraints.
2) Vary one parameter of the model, such as the base length (L1), and record the deflection and the peak stresses on a spreadsheet.
3) Repeat the above steps by next varying the thickness and then the outer diameter of the tube.
4) Analyze the frame again by adding triangulation of varying outer diameter (OD) and thicknesses.
5) Compare and contrast the results obtained in the spreadsheet to see the variance in stiffness to weight to the varying design parameters.
6) Take the existing values and simulate a Design of Experiments (DOE) in Hyperstudy to obtain Main effect plots and Interaction plots.

7) Use the DOE study to generate an approximation model for torsional/flexural stiffness and stresses for the various design variables.

1.4 Outline of the thesis

Chapter 1 describes a brief history and importance of an efficient chassis with the help of triangulation in the case of a space frame. It also shows the various types of chassis being used today.

Chapter 2 explains the various loads to be considered while design of the vehicle. It does so along with derivation of the equation to calculate torsional and flexural rigidity of the frame.

Chapter 3 talks about the use of Finite Element Method in solving the various node-element models created in ANSYS APDL and also show the procedure followed for obtaining the required results.

Chapter 4 refers to the use of Hyperstudy in order to generate a Design of Experiments (DOE) for the various design variables and responses and aims to extrapolate a mathematical model from the results.

Chapter 5 documents the results and graphical data obtained from Chapters 3 and 4 and also summarizes the findings of this thesis.

CHAPTER 2

LOADING OF THE CHASSIS

2.1 Introduction

In order to understand the need for efficient triangulation in a Formula SAE vehicle, we must first understand the various types of loads acting on it. These loads cases will provide a method to observe the variance seen in the frame design and also provide a basis for calculating the desired responses.

2.2 Deformation Modes

The loading on the chassis is brought about by the various maneuvers the vehicle makes on the track. These loads cases are described [5] as follows,

2.2.1 Longitudinal Torsion

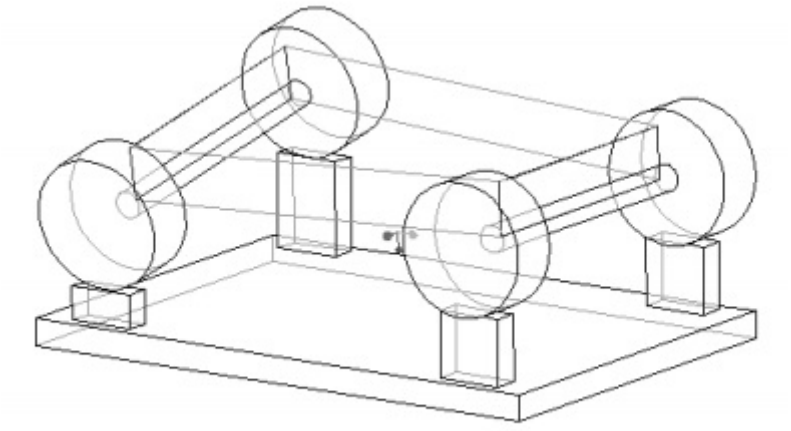

Figure 2.1 Chassis under Longitudinal Torsion

These loads are observed when the applied load is acting on either one or two oppositely opposed corners of the vehicle. These loads have a significant effect on the handling of the vehicle as the frame acts as a torsional spring connecting the two ends where the suspension loads act. Longitudinal Torsion is measured in foot-pounds per degree and is a primary factor for evaluating the efficiency of the frame. A detailed discussion on the calculation of this parameter is described later in this chapter.

2.2.2 Vertical Bending

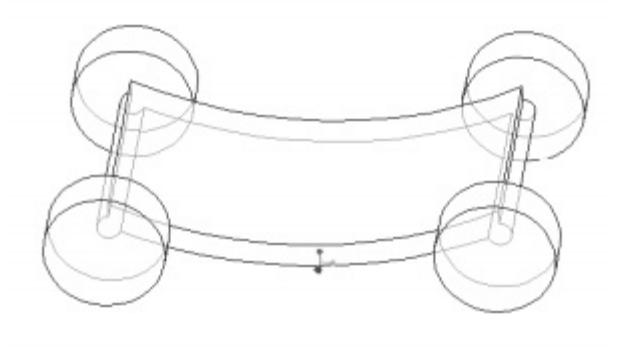

Figure 2.2 Chassis under Vertical Bending

Vertical bending is caused due to the vertical forces exerted on the frame due to gravity. In context to a Formula SAE car, the major contributors of the load include the driver and the engine. The application of these loads on the frame depends on the placement of afore mentioned contributors. The reactions of these loads are taken up at the axles and are affected by the vertical accelerations on the vehicle. These loads also aid in the determination of the frame stiffness.

2.2.3 Lateral Bending

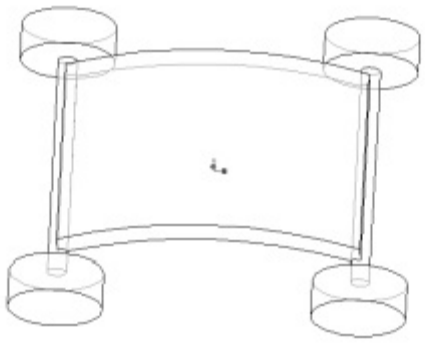

Figure 2.3 Chassis under Lateral Bending

Lateral bending is a result of the loads generated by road camber, side winds and mainly due to the centrifugal forces acting on the car during cornering. These loads act along the entire length of the car and are resisted at the tires.

2.2.4 Horizontal Lozenging

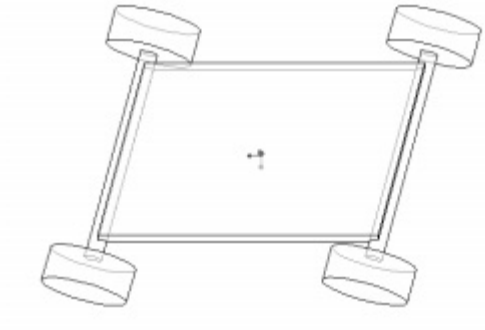

Figure 2.4 Chassis under Horizontal Lozenging.

This deformation is observed when the forward and backward forces are applied at opposite wheels. These loads cause the frame along the axles to bend which distorts the frame into a parallelogram. They are generally caused by road reaction on the tires while the car is moving forward.

Afore mentioned loading scenarios aid the analysis of the frame by aiming to minimize their effect. The torsional and bending loads in the longitudinal and vertical direction respectively are the major contributors to chassis deformation and thus are analyzed to improve the design.

2.3 Load Paths

This section is to describe the importance of load paths while designing a frame. The triangulation members in the frame of a Formula SAE car are not only used add stiffness to the vehicle but also provide significant area to accommodate for the various loads acting on it. These loads result in the creation of bending, torsional and combined stress on the chassis. In order to minimize stress concentration and enable a more effecting load path, triangulation is added. The added triangulation either acts in tension or compression based on their geometry and orientation. The following figures were taken from [6] to depict the load paths on a stationary automobile.

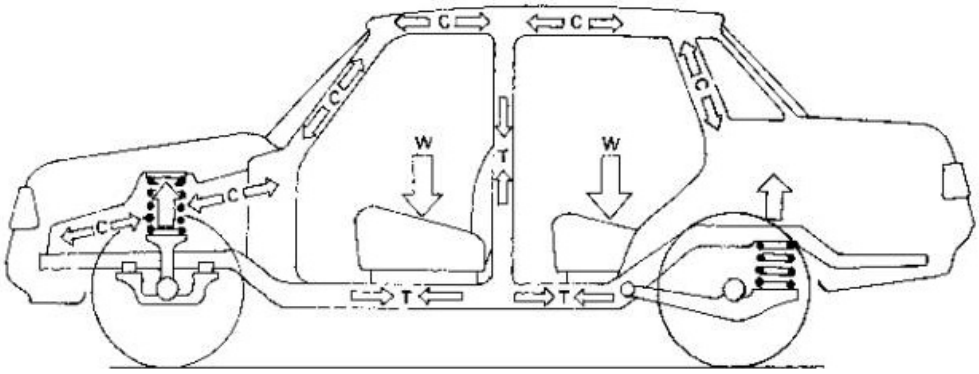

Figure 2.5 Lengthwise body loading

Here we can see the load paths acting on an automobile. The roof and base of the vehicle are under high stress and hence these areas need to be considerably strong.

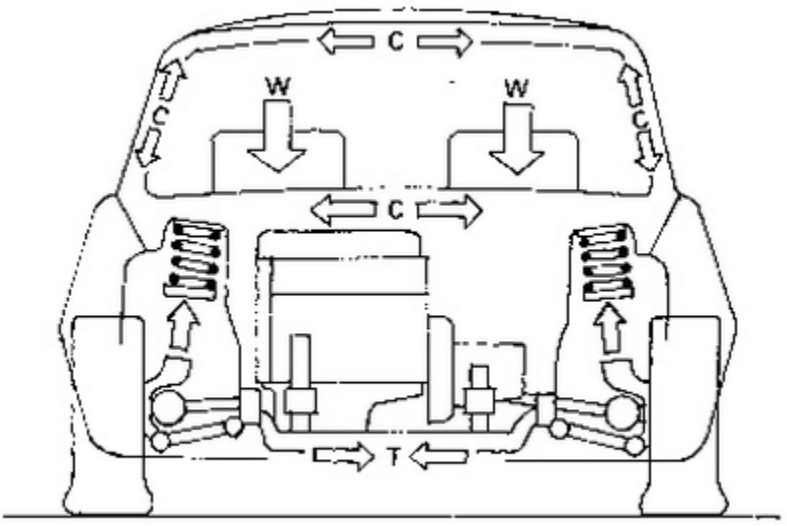

Figure 2.6 Transverse body loading

These load paths are similar in a Formula SAE race car and hence the roll hoops are designed to withstand higher loads and the floor of the car is well triangulated. The load paths give a better understanding on how to design the frame. The critical areas are always in close proximity to where maximum load in carried and the suspension pick up points. These areas need to be well triangulated to dissipate the stresses and also stiffen the frame.

2.4 Torsional Rigidity

Let us consider a beam element in 3D space to demonstrate the various forces and displacements acting on it. This element can be easily compared to the car in terms of loading applied and hence aid in the formulation of an expression for torsional rigidity. The term force is used to denote both forces and moments and displacement is used to denote both translational and rotational displacements. [7]

The generalized forces and displacements are as follows,

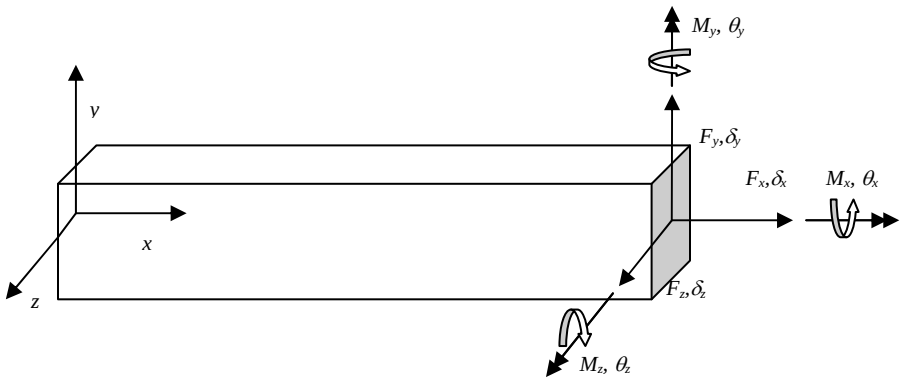

Figure 2.7 Forces and Moments of a Generalized Beam

This figure represents the various forces and displacements that can be applied on a general beam element. The forces and moments create bending and torsional loads on the beam. The forces along the x-axis induce tension or compression based on the direction while the forces along the y and z axes induce bending in the xy and xz plane respectively. Similarly the moment about the x-axis induces torsion in the beam whereas the other two moments result in bending. These generalized forces and displacements can be written as shown below,

$$\begin{bmatrix} f_1 \\ f_2 \\ f_3 \\ f_4 \\ f_5 \\ f_6 \end{bmatrix} = \begin{bmatrix} F_x \\ F_y \\ F_z \\ M_x \\ M_y \\ M_z \end{bmatrix}, \begin{bmatrix} \delta_1 \\ \delta_2 \\ \delta_3 \\ \delta_4 \\ \delta_5 \\ \delta_6 \end{bmatrix} = \begin{bmatrix} \delta_x \\ \delta_y \\ \delta_z \\ \theta_x \\ \theta_y \\ \theta_z \end{bmatrix}$$

In order to evaluate the effects of torsion on the beam along the x-axis, the moment and angular deflection about that axis is to be considered. Hence the torsional rigidity or torsional stiffness can be defined as the ratio of the moment to the amount of angular deflection in the beam and is written as follows,

$$K = \frac{Mx}{\theta x}$$

Where,

K = Torsional Rigidity of the beam

Now, for calculating the torsional rigidity of the chassis, the following model is considered

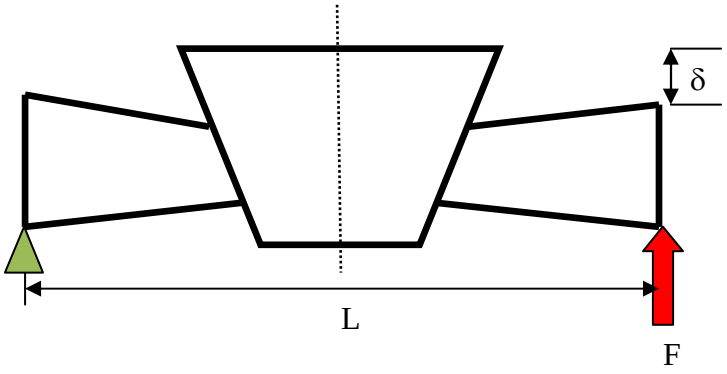

Figure 2.8 Torsional loading of the front of the chassis

The diagram represents the front of the chassis with the loads and boundary conditions applied to the front uprights (which connect the upper and lower suspension control arms of the suspension) and cause a twisting moment on the frame. The deflection 'δ' of the upright due to the force 'F' is measured in order to calculate the torsional rigidity given by the following equation,

$$Torque = T = \frac{F.L}{12}\ [lb.ft]$$

$$Angle = \ \theta = \tan^{-1}\left(\frac{\delta}{L}\right)\ [deg]$$

$$Torsional\ rigidity = K = \frac{T}{\theta} = \frac{F.L}{\tan^{-1}\left(\frac{\delta}{L}\right)} \times \frac{1}{12}\ [\frac{ft.lb}{deg}]$$

Where,

F = Force on the upright (lb)

δ = Maximum Deflection (in)

L = Track width/distance between the front wheels (in)

2.5 Flexural Rigidity

The flexural rigidity can be calculated in a similar manner shown above. Let us consider a simply supported beam in this case having a point load which is equidistant from either end. The illustration is shown below,

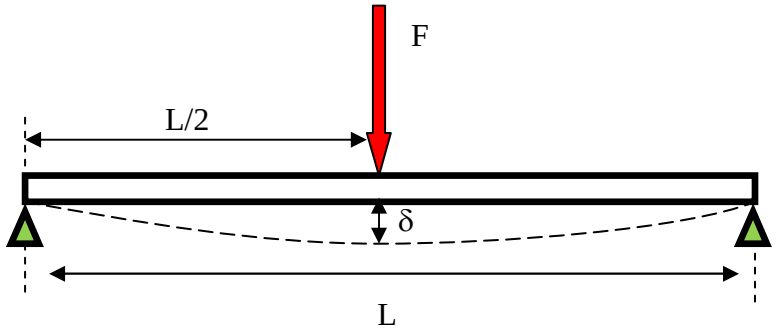

Figure 2.9 Flexural loading of a beam

The maximum deflection for a simply supported bar with a point load at the centre of the beam is given by,

$$Max.Deflection \; = \; \delta = \frac{FL^3}{48EI} \; [in]$$

$$Flexural \; stiffness = \frac{F}{\delta} \; [\frac{lb}{in}]$$

Where,

EI = Flexural Rigidity (lb.in^2)

F = Force applied (lb)

L = Length of the beam (in)

δ = Maximum deflection at the center (in)

The flexural stiffness of the frame can be computed in a similar way as the bulk of the static load, such as driver and engine weight, act close to the center of gravity (CG) of the car.

The position of the CG of the car depends on the type of weight bias is to be set for the car and hence it may travel forward/backward of the CG plane.

Generally the flexural rigidity of the space frame is quite high and is not a crucial component of the frame design. If the chassis is well triangulated to withstand sufficient torsional loads then it will be sufficiently stiff in bending. [8]

2.6 The power function – "Rules of Thumb"

As described by Crispin Mount Miller [9], for a torsional or flexural load, the rigidity of a tube is dependent on its moment of inertia and the strength is dependent on the section modulus which is the ratio of the moment of inertia to the distance between the neutral axis and the farthest element of the cross section. This theory brings about the following rules of thumb (approximations) for a tube undergoing torsional and bending loads.

1. If the OD and wall thickness are multiplied by a factor 'k', then the rigidity increases by a factor of k^4 and the strength increases by a factor of k^3 while the weight increases by k^2.
2. For no change in the wall thickness and the OD is multiplied by a factor 'k', then the rigidity increases by a factor of k^3 and the strength by k^2 while the weight increases by k.
3. If the OD is multiplied by 'k' but the thickness is divided by a factor 'k', then the rigidity increase by a factor of approximately k^2 and the strength by a factor of k. the weight in this case stays approximately the same.
4. If the OD remains the same and the thickness alone is multiplied by a factor of 'k', then both torsional and bending rigidities along with the strength and weight increase by a factor of k.

These approximations are reasonably true for thin walled tubes. Also approximations 2 and 3 have some limitations as the tubes may become too thick or thin.

CHAPTER 3

FINITE ELEMENT METHOD USING ANSYS 13.0

3.1 Introduction

The concept of finite element method is to break down a given model into smaller elements which are interconnected by two or more nodes/surfaces. These elements are analyzed using basic mathematical theory and then grouped together in the form of a matrix to give accurate outputs. The implementation of finite element method is mathematically complex as it requires the solution of large matrices which take up a large amount of computational time. Hence, Finite element method is a numerical method for solving problems involving complex geometries, loadings and material properties in engineering design. [10]

3.2 Basic understanding of Finite Element Method

The following example of a linear spring will aid us in understanding the FEA process. The spring is represented as follows,

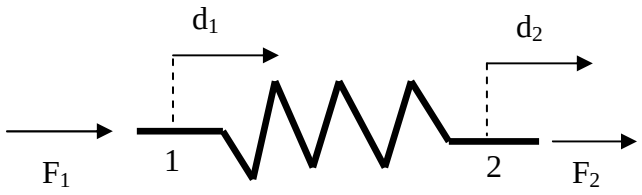

Figure 3.1 Spring element

The spring is called an element and has 2 degrees of freedom in the x direction at each node. Assuming positive displacements, the sum of the forces at F_1 an F_2 can be given by,

$$F_1 = kd_1 - kd_2$$

$$F_2 = -kd_1 + kd_2$$

Where,

K = Stiffness of the spring element

d_1, d_2 = Displacements at node 1& 2 respectively

F_1, F_2 = Forces at nodes 1& 2 respectively

Substituting these equations in matrix form,

$$\begin{bmatrix} k & -k \\ -k & k \end{bmatrix} \begin{Bmatrix} d_1 \\ d_2 \end{Bmatrix} = \begin{Bmatrix} F_1 \\ F_2 \end{Bmatrix}$$

$$[K]\{d\} = \{F\}$$

Where,

K = Stiffness matrix

d = Displacement vector

F = Force vector

Similarly, if there are two springs A &B connected in series, their equivalent stiffness matrix can be calculated and analyzed by applying the boundary conditions to the generalized equation.

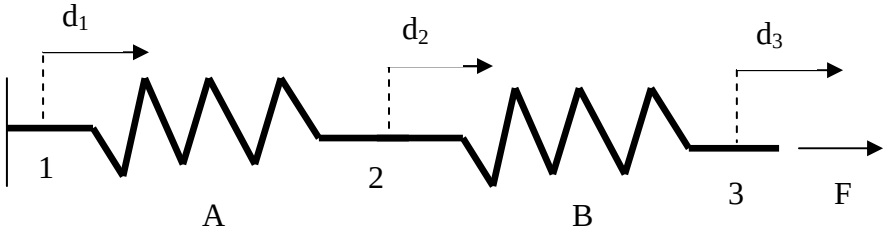

Figure 3.2 Spring element in series

The resultant matrix form is given by,

$$\begin{bmatrix} k_A & -k_A & 0 \\ -k_A & k_A + k_B & -k_B \\ 0 & -k_B & k_B \end{bmatrix} \begin{Bmatrix} d_1 \\ d_2 \\ d_3 \end{Bmatrix} = \begin{Bmatrix} F_1 \\ F_2 \\ F_3 \end{Bmatrix}$$

For the details of the derivation of this equation, refer [11]

Once we calculate the global stiffness matrix and substitute in the generalized equation, we can solve for unknown variables by substituting the known variables and solving the set of simultaneous equations. This method can be extremely time consuming and challenging for systems with infinite springs and thus requires sufficient computing power.

In this way, Finite Element Method converts a solid model into smaller spring elements and calculates the individual deflections and solves the overall matrix solution to give accurate results.

3.3 Design methodology

3.3.1 Torsional stiffness study

In order to characterize the various design variables and their effects on the response of a system, the model must be simple in design and must have clear visual representation of the response. In the case of an automotive chassis, the amount of tubes and various members result in a complex and bulky design. Hence in order to simplify the design for a torsional study, let's consider a rectangular section which is created by hollow thin walled tubes welded together.

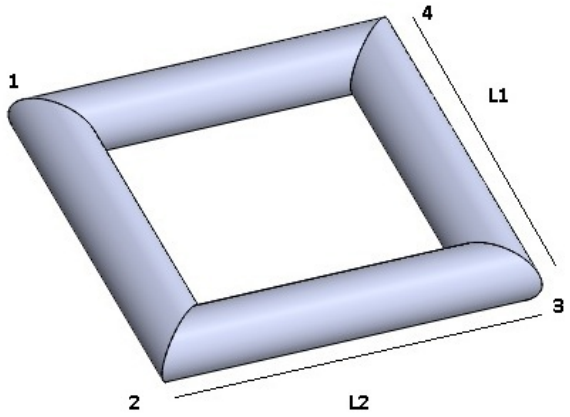

Figure 3.3 Rectangular section of welded tubes

The node-element model is created in ANSYS APDL using a Beam 188 element. We define the material as 4130 chromoly steel by entering the material properties of the same. The section properties of the element can be defined and is taken as a hollow cylinder to represent the tube having an outer diameter of 1 inch and thickness of 0.028 inches (1028) for the first set of design variables. The cross section of the steel tube is shown below,

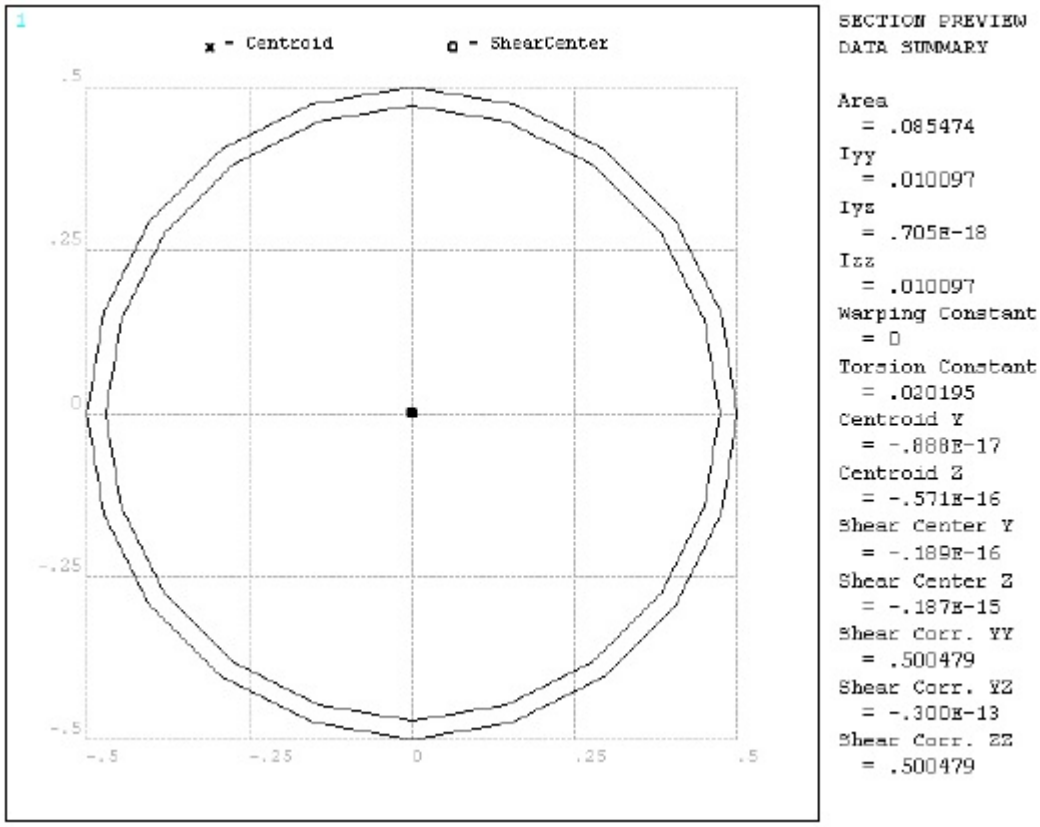

Figure 3.4 Cross-section(c/s) of tubes in ANSYS

These rectangular sections are created as node-element models in ANSYS APDL and the constraints are applied. In order to setup an FEA for a torsion test, without over constraining the model, the following constraints are applied,

1. The node diagonally opposite to the load in constrained in X, Y, and Z directions in terms of displacements.
2. The node adjacent to it (either one) is restrained from translating in the X and Y directions.
3. The other node is fixed in vertical displacement i.e., Y direction.

By constraining the model as specified above, we prevent motion of the object in its rigid body modes. If these 6 rigid body modes are not constrained, the global stiffness matrix becomes singular and hence cannot be solved. [12] A visual representation of the constraints is shown below.

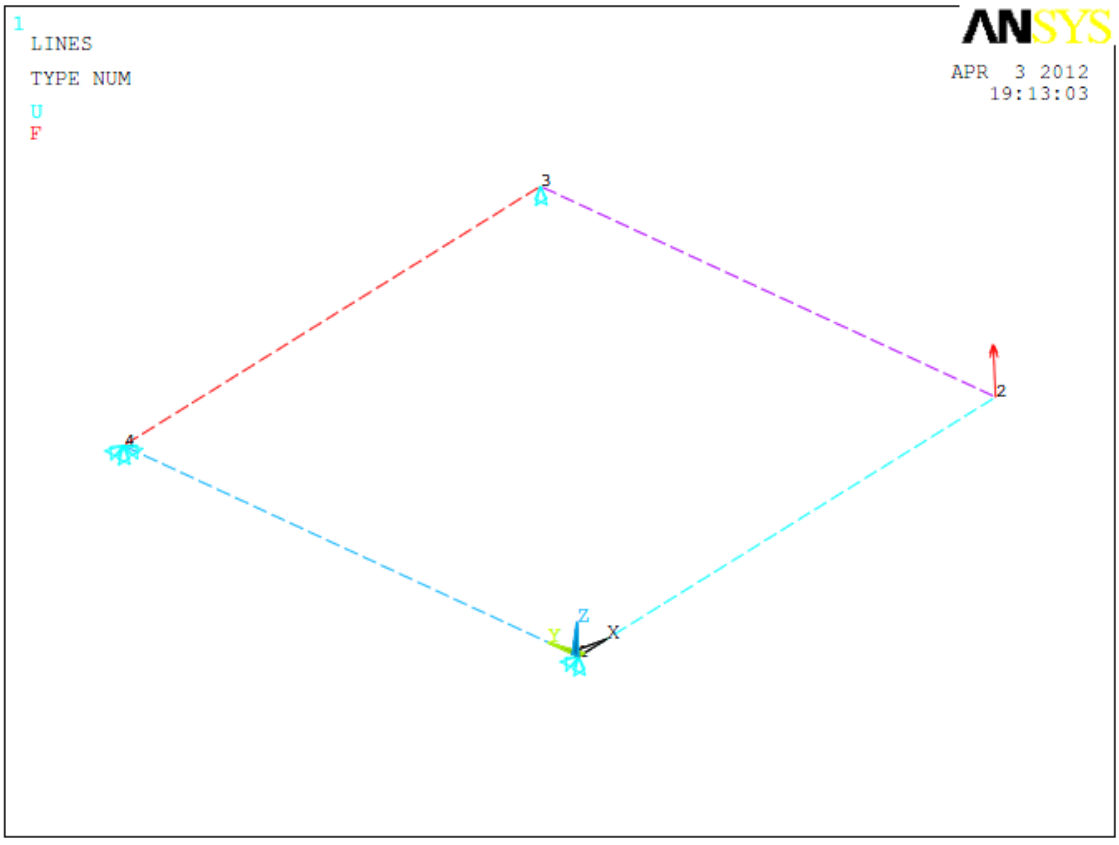

Figure 3.5 Constraints and forces for torsional case

Once the constraints are applied, a 100 lb load is applied as shown in the figure above. In case of a torsional study, the stiffness is a function of both the load and the deflection it induces. Hence the load can be any significant amount which would produce measureable deflection. The load is a factor when we check for stress in the structure which is not part of the estimation of torsional rigidity.

The model is now well constrained to run the FEA for torsional rigidity. The following deformation and stresses are observed,

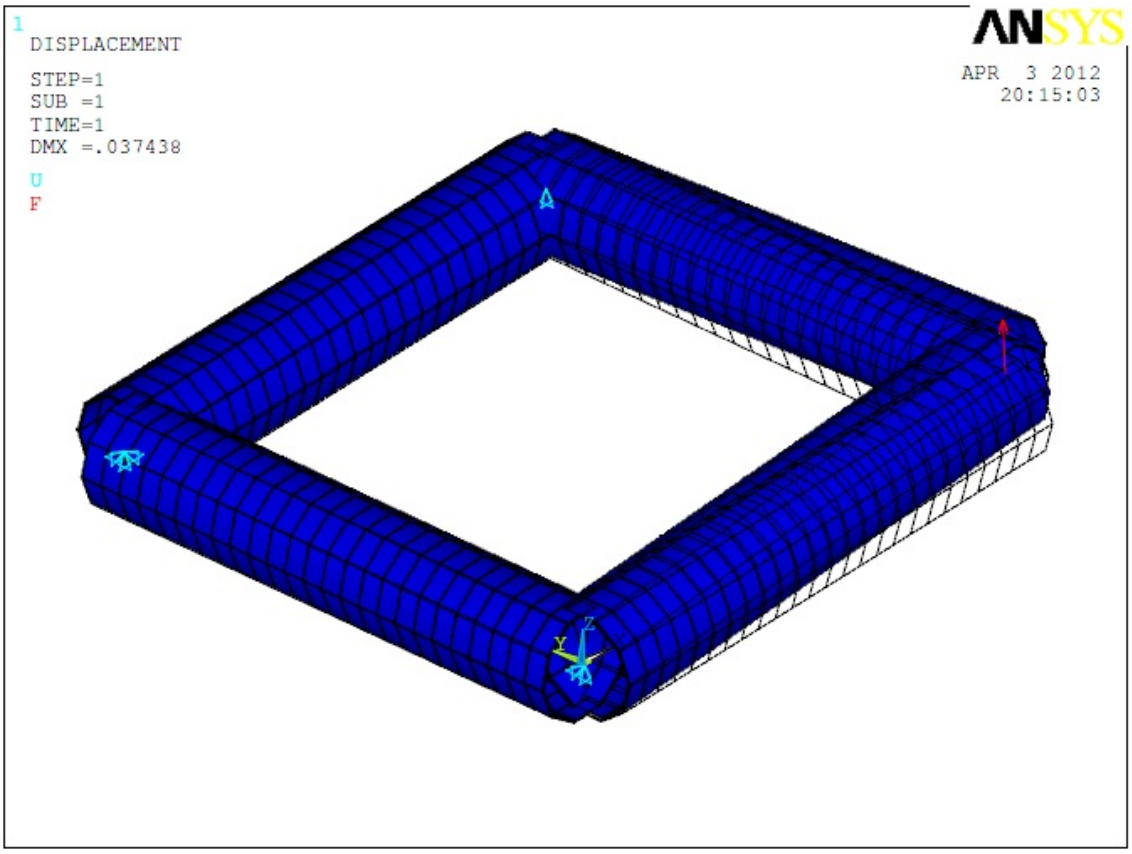

Figure 3.6 Displacement of rectangular section

The maximum deflection in the frame for a 100 lb load was 0.0374 inches and the maximum von mises stress recorded is 14934 psi or 14.93 ksi. As can be seen from the figure below, the maximum stress concentration is at the nodes. The nodes are stronger as they are

reinforced by welding to tubes together and are the best location to form load paths in order to transfer the load.

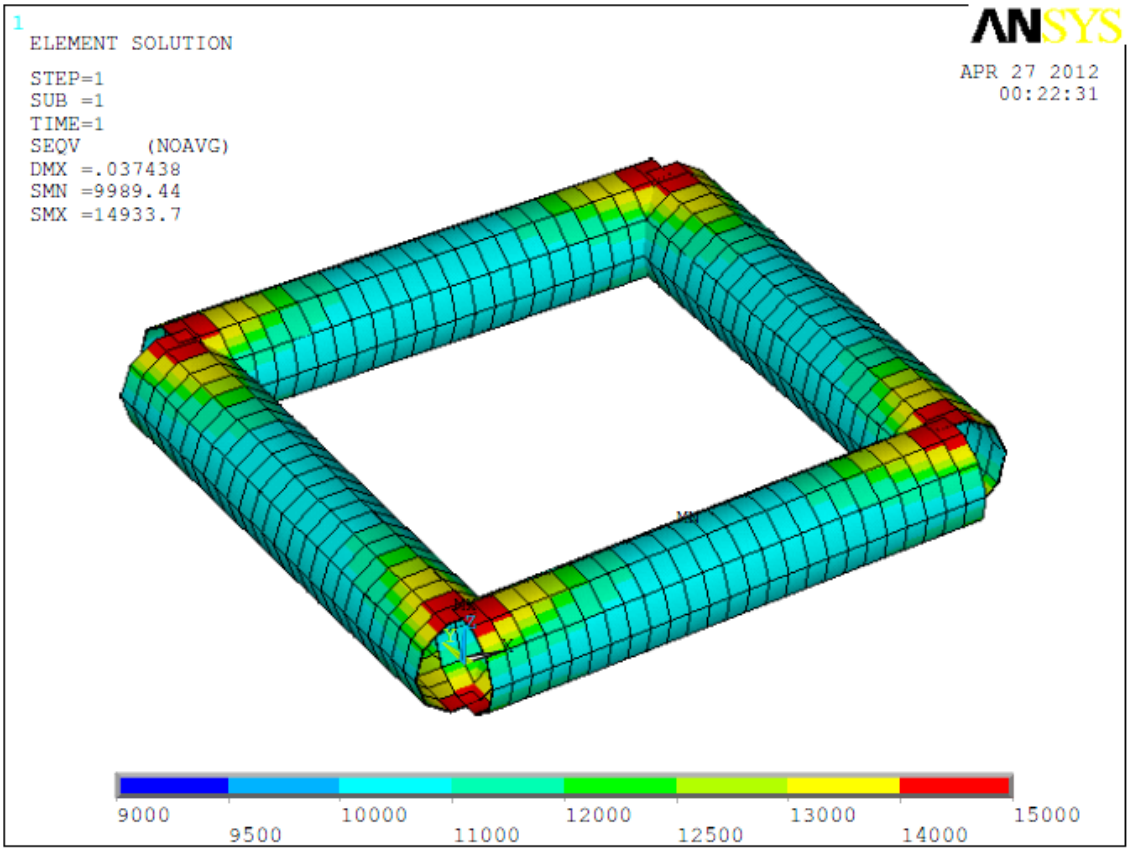

Figure 3.7 Stress distribution of rectangular plate

3.3.1.1 Stiffness calculation

Now calculating the torsional stiffness of the structures from the deflection observed in the model,

$$Torsional\ rigidity = K = \frac{T}{\theta} = \frac{F.L}{\tan^{-1}\left(\frac{\delta}{L}\right)} \times \frac{1}{12}\ [\frac{ft.lb}{deg}]$$

Where,

$F = 100\ \text{lb}\ ;\ L = 5\ \text{in}\ ;\ \delta = 0.037438\ \text{in}$

$$K = \frac{100 * 5}{\tan^{-1}\left(\frac{0.037438}{5}\right)} * \frac{1}{12}$$

$$K = 97.22\ ft.lb/deg$$

Similarly, the deflection is recorded by varying the length in the X direction. These values are then entered in a spread sheet which also calculates the weight of the structure to give the stiffness to weight ratio. The weight is calculated by multiplying the volume of the structure with the density of the material. The following table shows the stiffness to weight ratio's calculated for varying length L_1.

Table 3.1 Stiffness to weight variation for 1" OD X 0.028" thickness (Torsional)

Sr. No.	Base Length L_1 (in)	Load (lb)	Deflection (in)	Stiffness (ft lb/deg)	Weight (lb)	Stiffness to weight ratio (ft/deg)
1	5	100	0.0374	97.22	0.245	396.096
2	7.5	100	0.0658	55.26	0.307	180.116
3	10	100	0.0956	38.04	0.368	103.316
4	12.5	100	0.1258	28.91	0.430	67.303
5	15	100	0.1561	23.30	0.491	47.465
6	17.5	100	0.1863	19.53	0.552	35.357
7	20	100	0.2164	16.81	0.614	27.399
8	22.5	100	0.2463	14.77	0.675	21.889
9	25	100	0.2761	13.18	0.736	17.903
10	27.5	100	0.3057	11.91	0.798	14.929
11	30	100	0.3353	10.86	0.859	12.642
12	32.5	100	0.3647	9.99	0.920	10.851
13	35	100	0.3941	9.25	0.982	9.417
14	37.5	100	0.4234	8.61	1.043	8.252
15	40	100	0.4526	8.06	1.105	7.293
16	42.5	100	0.4817	7.57	1.166	6.494
17	45	100	0.5108	7.14	1.227	5.820
18	47.5	100	0.5398	6.76	1.289	5.247
19	50	100	0.5687	6.42	1.350	4.756
20	52.5	100	0.5977	6.11	1.404	4.354

The same procedure was carried out for the following tube sizes,

- 1” OD X 0.049” thickness circular tube - 1049
- 1” OD X 0.065” thickness circular tube - 1065
- 1” OD X 0.095” thickness circular tube - 1095
- 5/8” OD X 0.035” thickness circular tube - 58035
- 1/2” OD X 0.028” thickness circular tube - 05028

The following graph shows the variation of stiffness with the base length (L_1) and linearized stiffness to weight ratio with respect to the ratio of the sides of the rectangle (L_1/L_2).

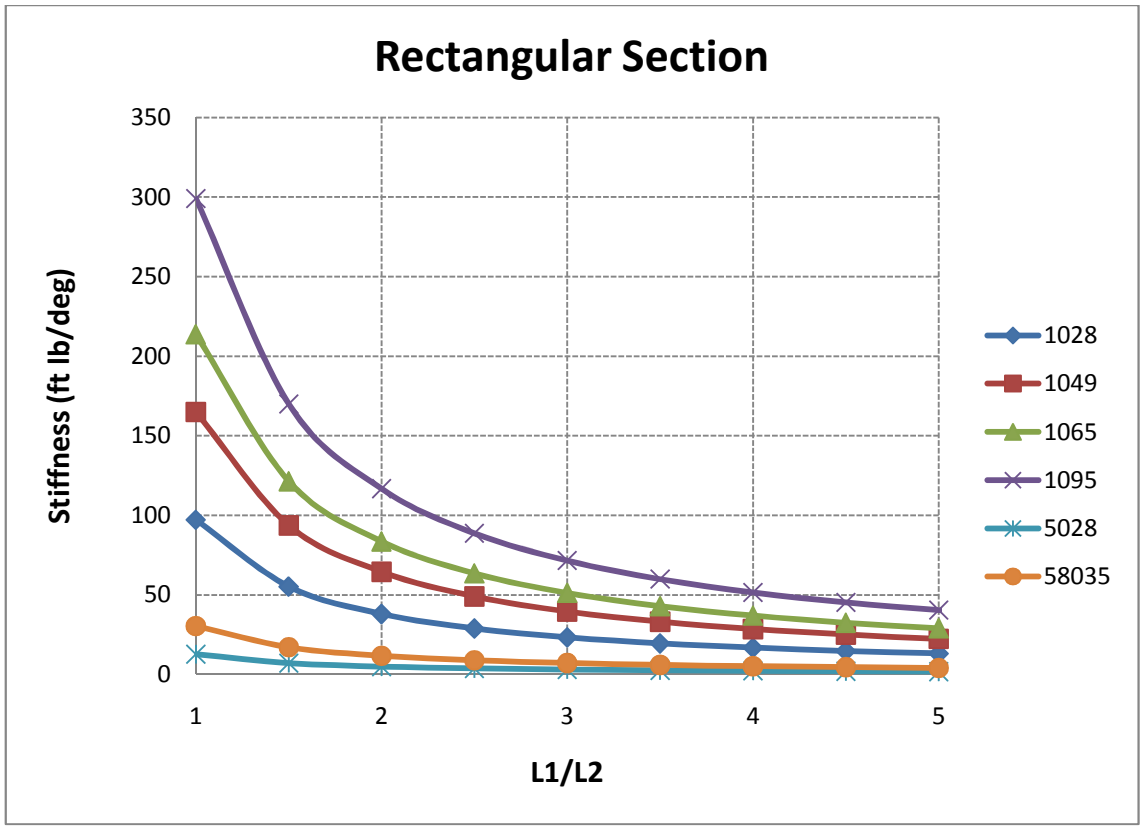

Figure 3.8 Graphical representation of stiffness vs. length ratio

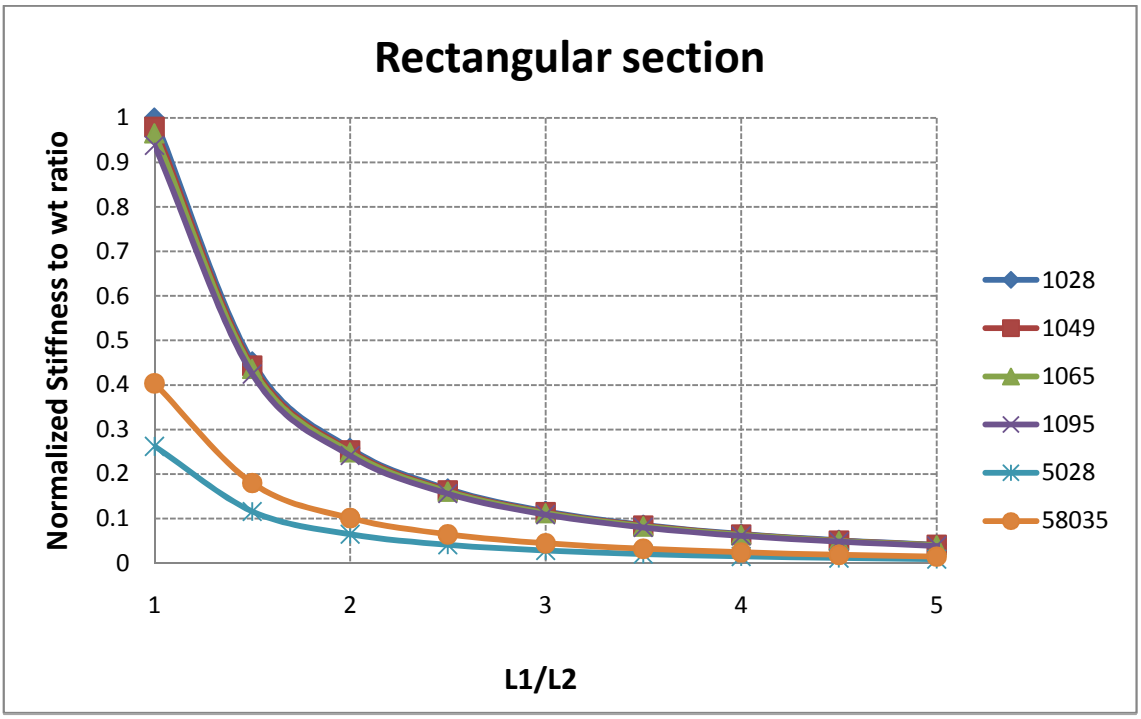

Figure 3.9 Graphical representation of normalized stiffness to weight vs. length ratio

As can be seen from the graph, for a torsional loading scenario, the thickness of the tube has negligible gain in stiffness to weight ratio whereas the OD of the tubes has a significant effect on the stiffness to weight ratio. The graph also depicts that for a L_1/L_2 ratio of 4 and above, the gain in stiffness to weight ratio is negligible.

3.3.1.2 Stress calculation

The Von Mises stresses in the structure for varying the design parameters are as follows,

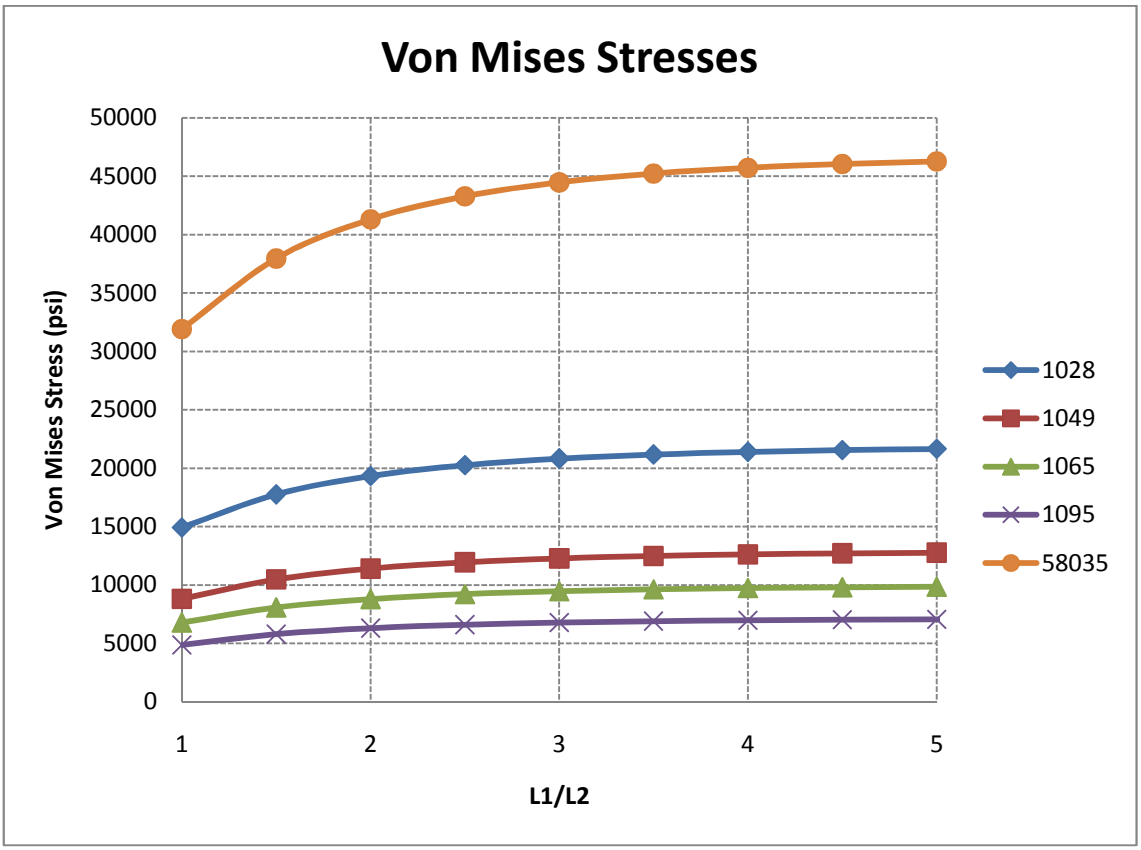

Figure 3.10 Graphical representation of Von Mises stresses vs. length ratio

The stress variance for ½" OD X 0.028" thickness tube is not included as the structure yields at the initial L1/L2 ratio. Hence it is excluded from the stress analysis.

According to the Power Function approximations, the torsional stiffness for a given ratio of L1 and L2 can be calculated using the "Rules of Thumb".

Applying rule 4,

Comparing 1028 and 1049 tubes in terms of stiffness,

$$k = \frac{0.049}{0.028} = 1.75$$

For 1028, Torsional stiffness at L1/L2 = 1, K_{1028} = 97.22 ft lb / deg

For 1049, Torsional stiffness at L1/L2 = 1, K_{1049} = 164.87 ft lb / deg

Therefore, for stiffness to increase by a factor of k = 1.75

k * K_{1028} = 1.75 * 97.22 = 170.135 ft lb / deg ≅ K_{1049}

The error is given by,

$$e = \left(\frac{170.135 - 164.87}{164.87}\right) * 100 = 3.19\%$$

Comparing 1028 and 1049 tubes in terms of stresses,

For 1028, Von Mises stress at L1/L2 = 1, σ_{1028} = 14933.7 psi

For 1049, Von Mises stress at L1/L2 = 1, σ_{1049} = 8808.28 psi

Stress reduces by a factor of k = 1.75

σ_{1028} / k = 14933.7 / 1.75 = 8533.54 psi ≅ σ_{1049}

The error is given by,

$$e = \left(\frac{8533.54 - 8808.28}{8808.28}\right) * 100 = -3.1\%$$

Applying rule 2,

Comparing 1028 and 05028 tubes in terms of stiffness,

$$k = \frac{1}{0.5} = 2$$

For 1028, Torsional stiffness at L1/L2 = 1, K_{1028} = 97.22 ft lb / deg

For 05028, Torsional stiffness at L1/L2 = 1, K_{05028} = 12.69 ft lb / deg

Therefore, for stiffness to increase by a factor of $k^3 = 2^3 = 8$

k * K_{05028} = 8 * 12.69 = 101.52 ft lb / deg ≅ K_{1028}

The error is given by,

$$e = \left(\frac{101.52 - 97.22}{97.22}\right) * 100 = 4.42\%$$

The rule 2 cannot be applied for this comparison as the stresses with the 05028 tube exceed the yield stress of the material.

3.3.2 Bending stiffness study

In this study, the specimen shape is that of a rectangular box of welded tubes. This shape is more representative of the frame of a race car as it contains fore and aft sections on either side of the roll hoop. The frame of the car is designed such that the CG is low and near to the center of the chassis to minimize the effects due to weight transfer. It also depends on the position of the driver and the engine to obtain a 50:50 weight bias. The rectangular box, along with its various measurements, is shown below.

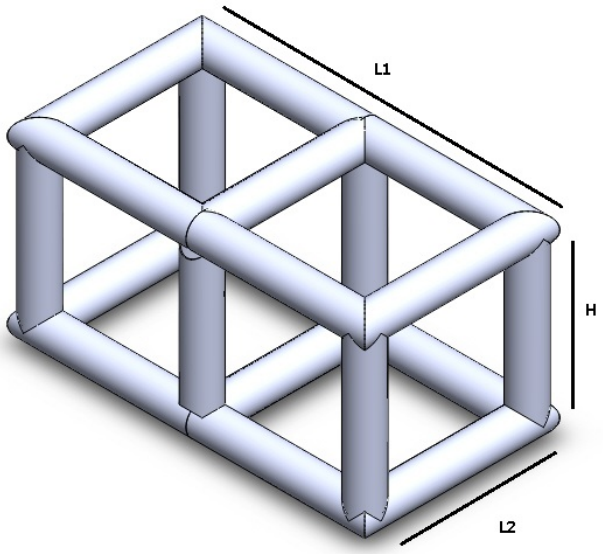

Figure 3.11 Rectangular box of welded tubes.

The rectangular box is constructed of the same size tube, 1” OD X 0.028” thickness, as in the case for torsional study and is varied each time. The constraints on the rectangular box is applied in a similar way as for the torsional case by making sure the 6 rigid modes of freedom are restrained and the model is simply supported at its ends. The load is applied to the mid-length of the rectangular box in order to simulate a bending load on the structure. This set up is shown in the figure below,

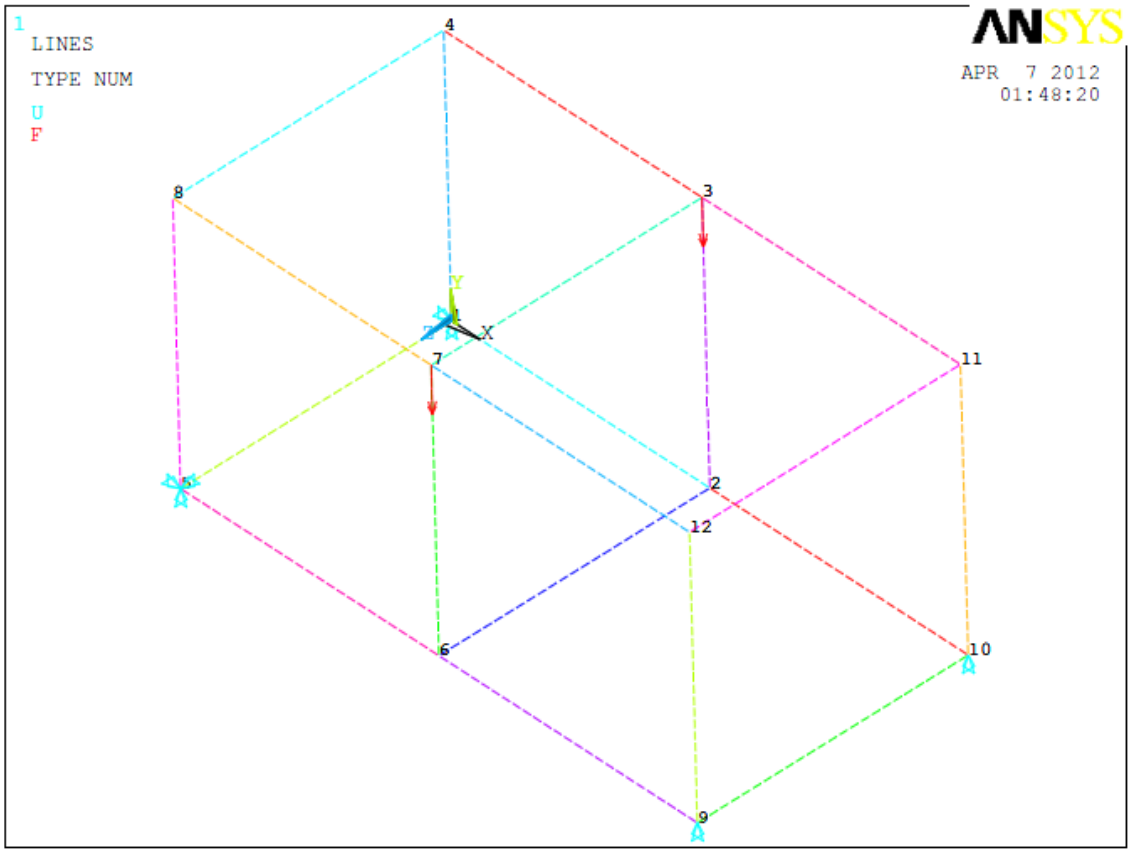

Figure 3.12 Constraints and forces for bending case

The magnitude of the load on each node is 100 lb which causes the frame to bend in the middle. The deflection and equivalent stresses in the structure are shown in figure 3.13 and figure 3.14 respectively. The max deflection is 3.26x10^-3 inches and the Von mises stress in the structure is 7390 psi.

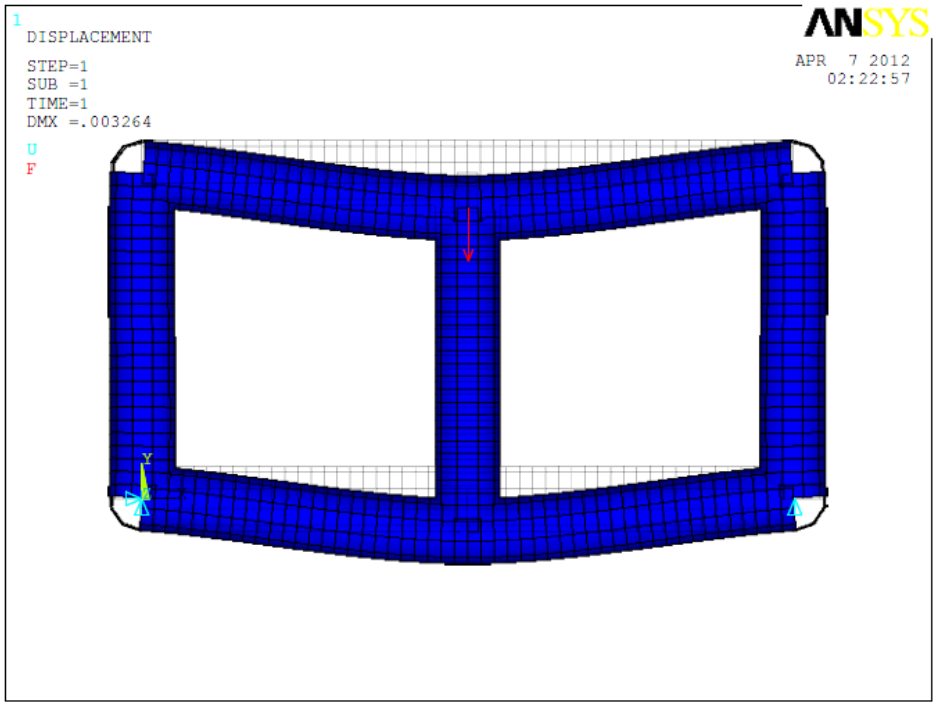

Figure 3.13 Displacement in bending case.

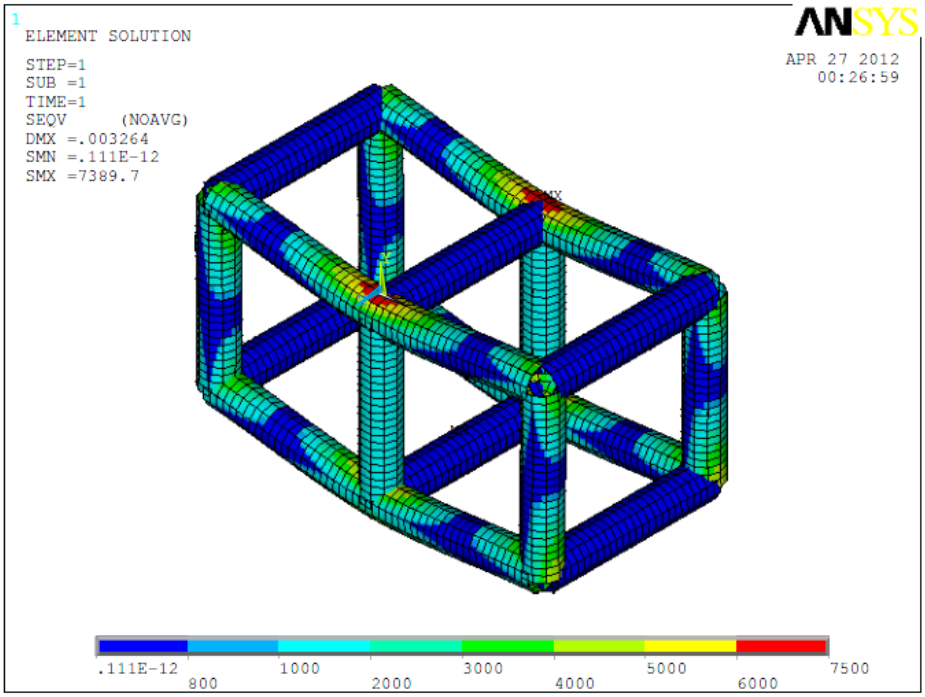

Figure 3.14 Stress distribution in bending case.

3.3.2.1 Stiffness calculation

Now calculating the bending stiffness of the structures from the deflection observed in the model,

$$Flexural\ stiffness = \frac{F}{\delta}\ [\frac{lb}{in}]$$

$$Bending\ stiffness = \frac{200}{0.00326} = 61349.69\ \frac{lb}{in}$$

This procedure is repeated by varying the length (L_1) while keeping L_2 and H constant. The resultant stiffness's are shown in the table below.

Table 3.2 Stiffness to weight variation for 1" OD 0.028" thickness (Flexural)

Sr. No.	Base Length (in)	Load (lb)	Deflection (in)	Flexural Stiffness (lb/in)	Weight (lb)	Stiffness to weight ratio (in^-1)
1	5	200	0.000796	251256.28	0.982	255908.47
2	10	200	0.00326	61349.69	1.227	49988.50
3	15	200	0.00888	22522.52	1.473	15293.02
4	20	200	0.0189	10582.01	1.718	6158.82
5	25	200	0.03489	5732.30	1.964	2919.21
6	30	200	0.0579	3454.23	2.209	1563.63
7	35	200	0.0893	2239.64	2.455	912.44
8	40	200	0.1306	1531.39	2.700	567.18
9	45	200	0.1829	1093.49	2.945	371.24
10	50	200	0.2476	807.75	3.191	253.14
11	55	200	0.326	613.49	3.436	178.53
12	60	200	0.4195	476.75	3.682	129.48

The same procedure is followed by varying the tube OD and thickness. The variation in the stiffness and also normalized stiffness to weight with respect to the ratio of the lengths (L_1/L_2) is shown in figures figure 3.14 and 3.15 respectively.

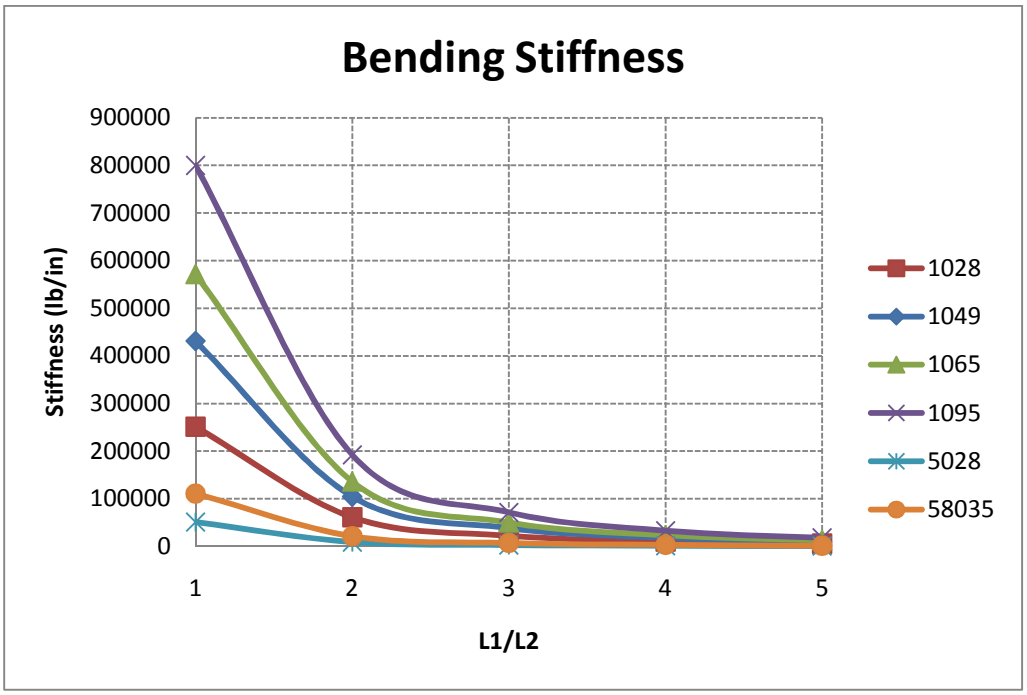

Figure 3.15 Graphical representation bending stiffness vs. length ratio

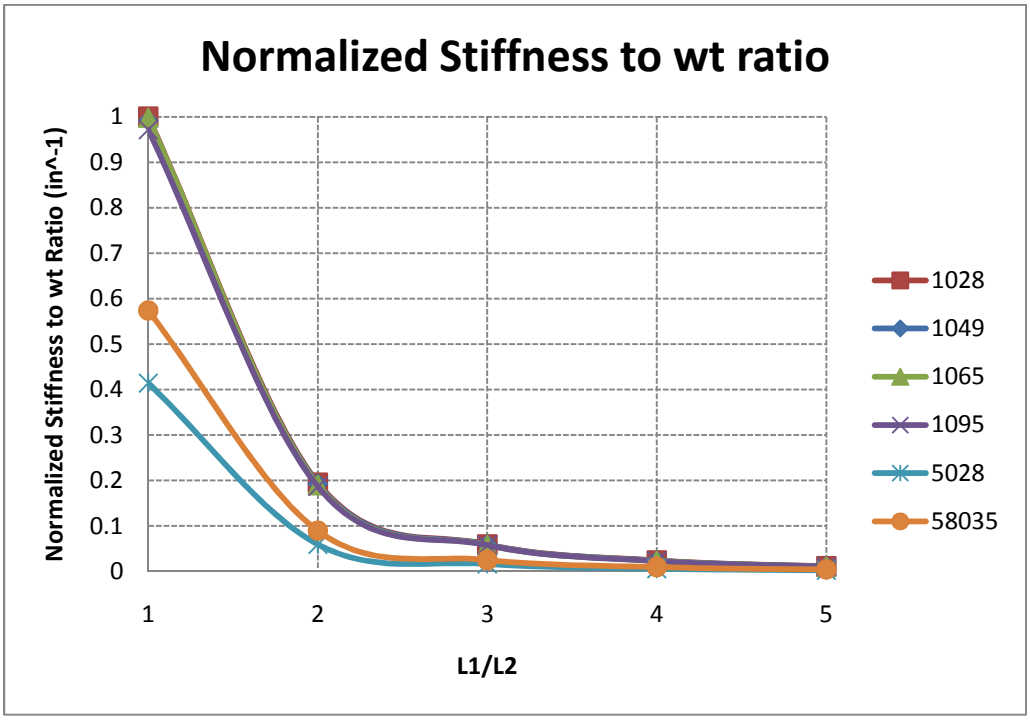

Figure 3.16 Graphical representation normalized stiffness to weight vs. length ratio

The stiffness to weight ratio for a bending load is not that different from the torsional case. The magnitude of stiffness is greater on a normalized scale as the structure has more weight in tubes. According to the data collected, the trend shows the effect on the stiffness to weight ratio diminishing at a faster rate and is negligible from an L1/L2 ratio of 2.

3.3.2.2 Stress calculation

The Von Mises stresses in the structure for varying the design parameters are as follows,

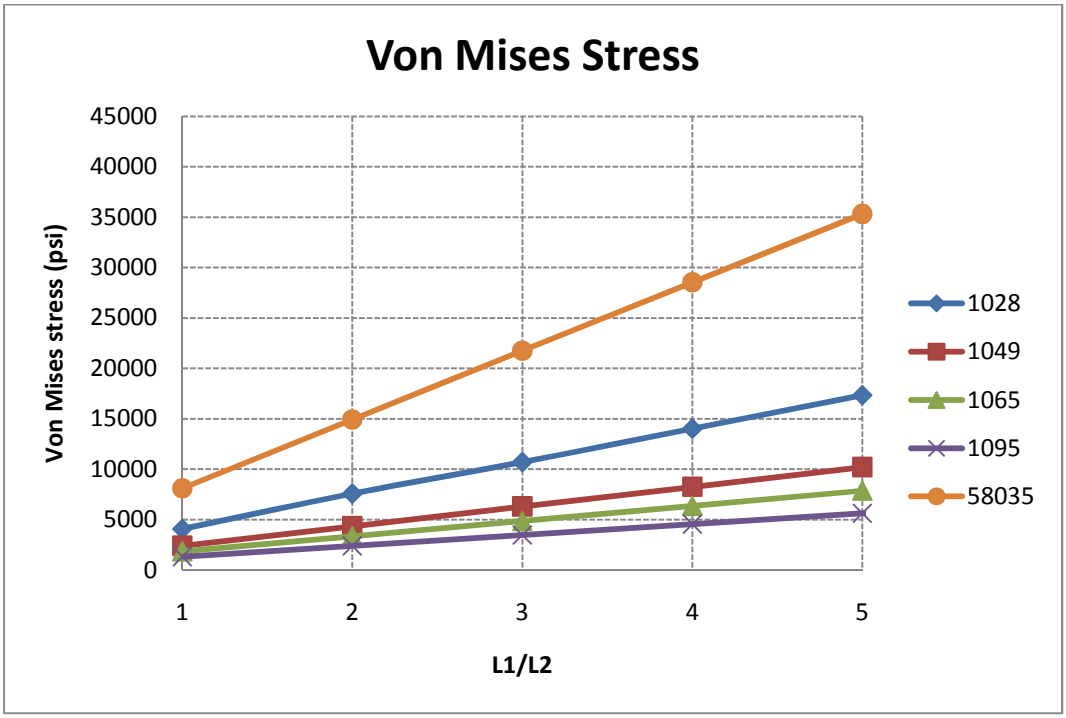

Figure 3.17 Graphical representation of Von Mises stresses vs. length ratio

The stress variance for ½" O.D X 0.028" thickness tube is not included as the structure yields at the initial L1/L2 ratio. Hence it is excluded from the stress analysis.

According to the Power Function approximations, the flexural stiffness for a given ratio of L1 and L2 can be calculated using the "Rules of Thumb".

Applying rule 4,

Comparing 1049 and 1065 tubes in terms of stiffness,

$$k = \frac{0.065}{0.049} = 1.326$$

For 1049, Torsional stiffness at L1/L2 = 1, K_{1028} = 431034.48 lb / in

For 1065, Torsional stiffness at L1/L2 = 1, K_{1049} = 571428.57 lb / in

Therefore, for stiffness to increase by a factor of k = 1.326

k * K_{1028} = 1.326 * 431034.48 = 571551.72 lb / in $\cong K_{1049}$

The error is given by,

$$e = \left(\frac{571551.72 - 571428.87}{571428.57}\right) * 100 = 0.021\%$$

Comparing 1049 and 1065 tubes in terms of stresses,

For 1049, Von Mises stress at L1/L2 = 4, σ_{1049} = 8255.96 psi

For 1065, Von Mises stress at L1/L2 = 4, σ_{1065} = 6366.04 psi

Stress reduces by a factor of k = 1.326

σ_{1049} / k = 8255.96 / 1.326 = 6226.21 psi $\cong \sigma_{1065}$

The error is given by,

$$e = \left(\frac{6226.21 - 6366.04}{6366.04}\right) * 100 = -2.19\%$$

Applying rule 2,

Comparing 1028 and 05028 tubes in terms of stiffness,

$$k = \frac{1}{0.5} = 2$$

For 1028, Torsional stiffness at L1/L2 = 3, K_{1028} = 5732.3 ft lb / deg

For 05028, Torsional stiffness at L1/L2 = 3, K_{05028} = 751.88 ft lb / deg

Therefore, for stiffness to increase by a factor of $k^3 = 2^3 = 8$

k * K_{05028} = 8 * 751.88 = 6015.04 ft lb / deg $\cong K_{1028}$

The error is given by,

$$e = \left(\frac{6015.04 - 5732.3}{5732.3}\right) * 100 = 4.9\%$$

The rule 2 cannot be applied for this comparison as the stresses with the 05028 tube exceed the yield stress of the material.

The stresses are dependent on the section modulus of the c/s which the ratio of the moment of inertia to the distance between the outer most element and the neutral axis.

$$\sigma = \frac{M * c}{I} = \sigma_y$$

$$M_{Yield} = \frac{\sigma_y * I}{c}$$

Where, $I = c^2 * \frac{\pi}{4} (D_o^2 - D_i^2)$

$c = Distance\ of\ the\ outermost\ element\ from\ the\ neutral\ axis$

Now since the frame is simply supported at its ends, the maximum moment is at the center and is given by

$$M_{max} = \frac{P * L}{4}$$

Where, $P = Load\ ; L = length\ of\ the\ frame$

Hence, we get

$$M_{max} = M_{Yield}$$

$$\frac{P * L}{4} = \frac{\sigma_y * I}{c}$$

$$L = \frac{4}{P} * \frac{\sigma_y * I}{c}$$

Hence for a given load we can calculate the length at which the structure will fail. Apply a factor of safety to the above equation to get the desired length of the rectangular section.

3.3.3 Linear stiffness study (Lateral bending)

Using the same model as above, the constraints and loads on the model are altered in order to evaluate the linear stiffness of the section. The model is now constrained in 2D space to generate a linear stiffness. Hence the following constraints need to be applied,

1. The node diagonally opposite to the load in constrained in X, Y, and Z directions in terms of displacements.
2. The node adjacent to it along the x-axis is restrained from translating in the Y direction and rotating about the x-axis.

A visual representation of the constraints is shown below.

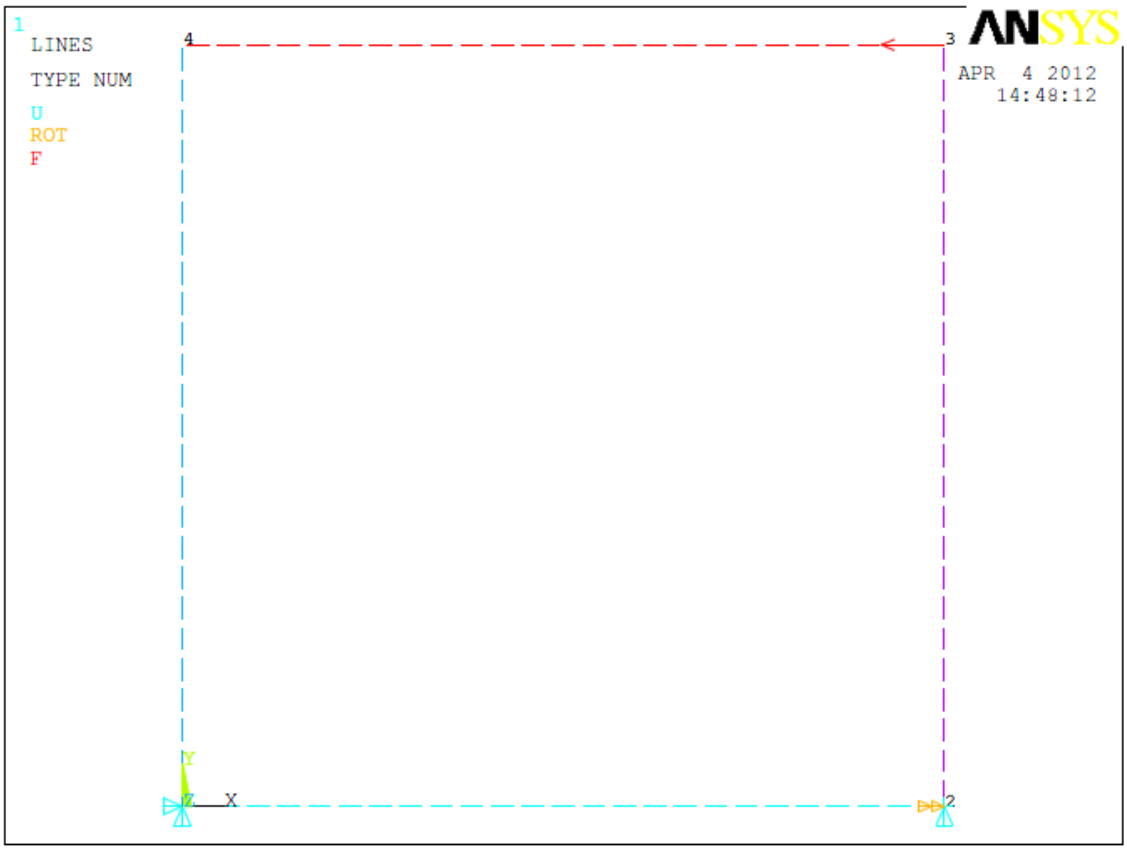

Figure 3.18 Constraints and forces for lateral bending case

The 100 lb load is applied along the X direction causing the structure to deform in the XY plane. The model is now well constrained to run the FEA for calculating linear stiffness. The following deformation and stresses are observed,

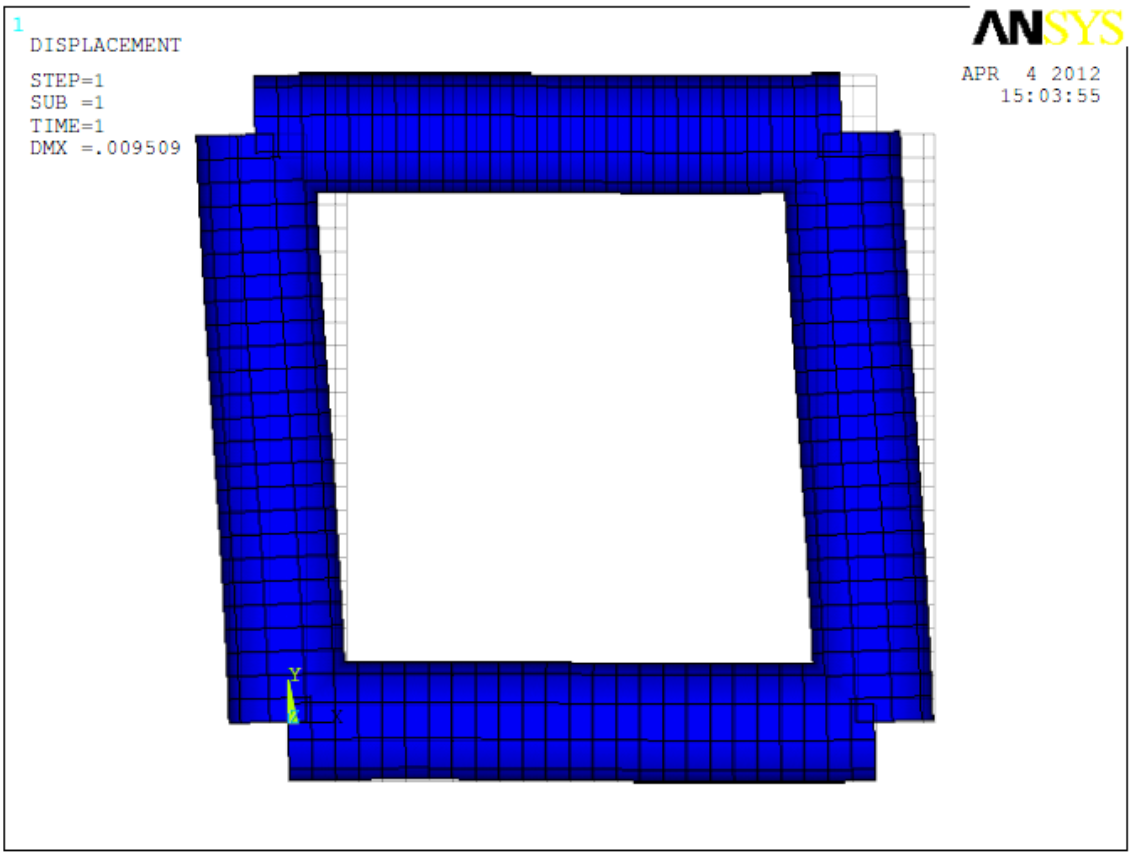

Figure 3.19 Displacement in lateral bending case

The maximum deflection in the frame for a 100 lb load was 0.0095 inches and the maximum Von Mises stress recorded is 12698 psi or 12.69 ksi.

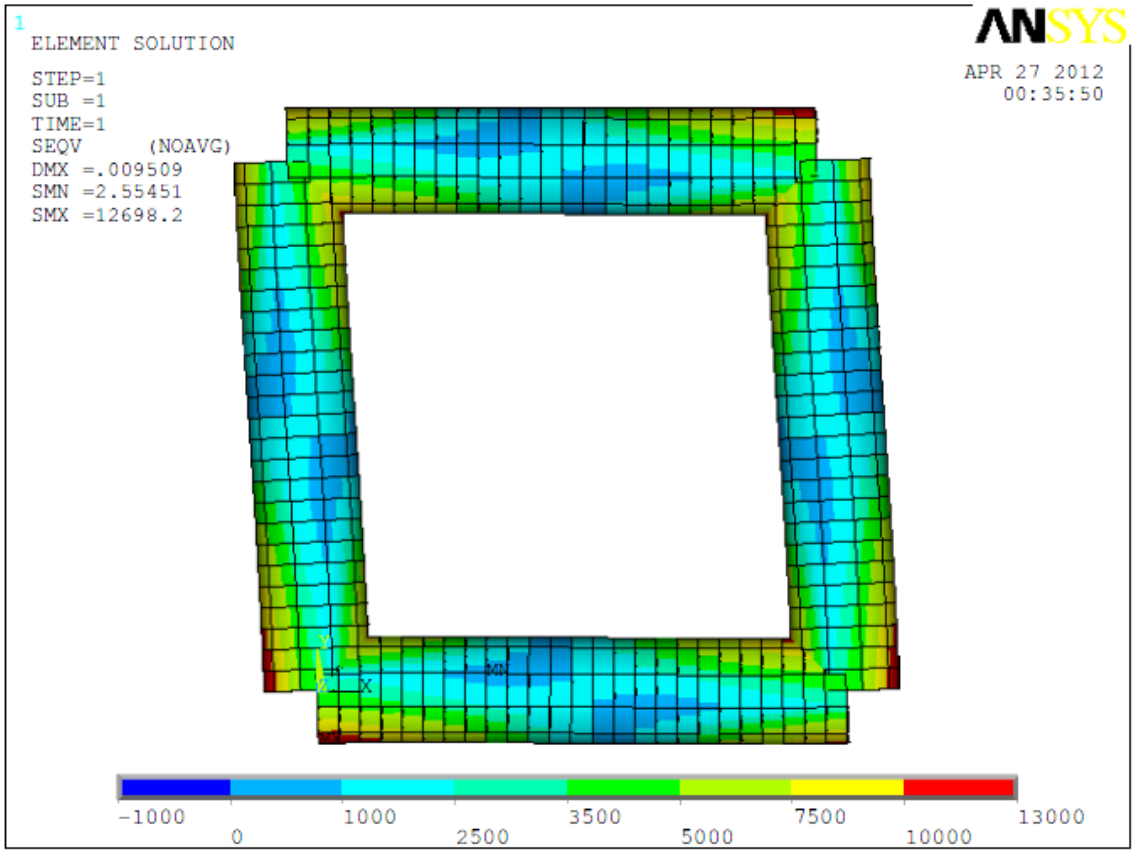

Figure 3.20 Stress Distribution in lateral bending case.

Similar to the procedure for torsional stiffness, the linear stiffness for varying lengths along y-axis L_1 are calculated in excel. A sample calculation is shown in the table below.

Table 3.3 Stiffness to weight variation for 1" OD 0.028" thickness (Linear)

Sr. No.	Base Length (L1)(in)	Load (lb)	Deflection (in)	Stiffness (lb/in)	Weight (lb)	Stiffness to weight ratio (in^-1)
1	5	100	0.0095	10526.32	0.245	42884.873
2	7.5	100	0.024	4166.67	0.307	13580.210
3	10	100	0.0486	2057.61	0.368	5588.564
4	12.5	100	0.086	1162.79	0.430	2707.019

Table 3.2 – *Continued*

5	15	100	0.1388	720.46	0.491	1467.602
6	17.5	100	0.209	478.47	0.552	866.361
7	20	100	0.301	332.23	0.614	541.404
8	22.5	100	0.415	240.96	0.675	356.983
9	25	100	0.556	179.86	0.736	244.248
10	27.5	100	0.725	137.93	0.798	172.905
11	30	100	0.926	107.99	0.859	125.704
12	32.5	100	1.16	86.21	0.920	93.657
13	35	100	1.43	69.93	0.982	71.225
14	37.5	100	1.74	57.47	1.043	55.092
15	40	100	2.09	47.85	1.105	43.318
16	42.5	100	2.48	40.32	1.166	34.585
17	45	100	2.93	34.13	1.227	27.809
18	47.5	100	3.42	29.24	1.289	22.690
19	50	100	3.97	25.19	1.350	18.658
20	52.5	100	4.57	21.88	1.404	15.585

The same procedure was carried out for the following tube sizes,

- 1” OD X 0.049” thickness circular tube - 1049
- 1” OD X 0.065” thickness circular tube - 1065
- 1” OD X 0.095” thickness circular tube - 1095
- 5/8” OD X 0.035” thickness circular tube - 58035
- 1/2” OD X 0.028” thickness circular tube - 05028

The following graph shows the variation of stiffness with the base length (L_1) and linearized stiffness to weight ratio with respect to the ratio of the sides of the rectangle (L_1/L_2).

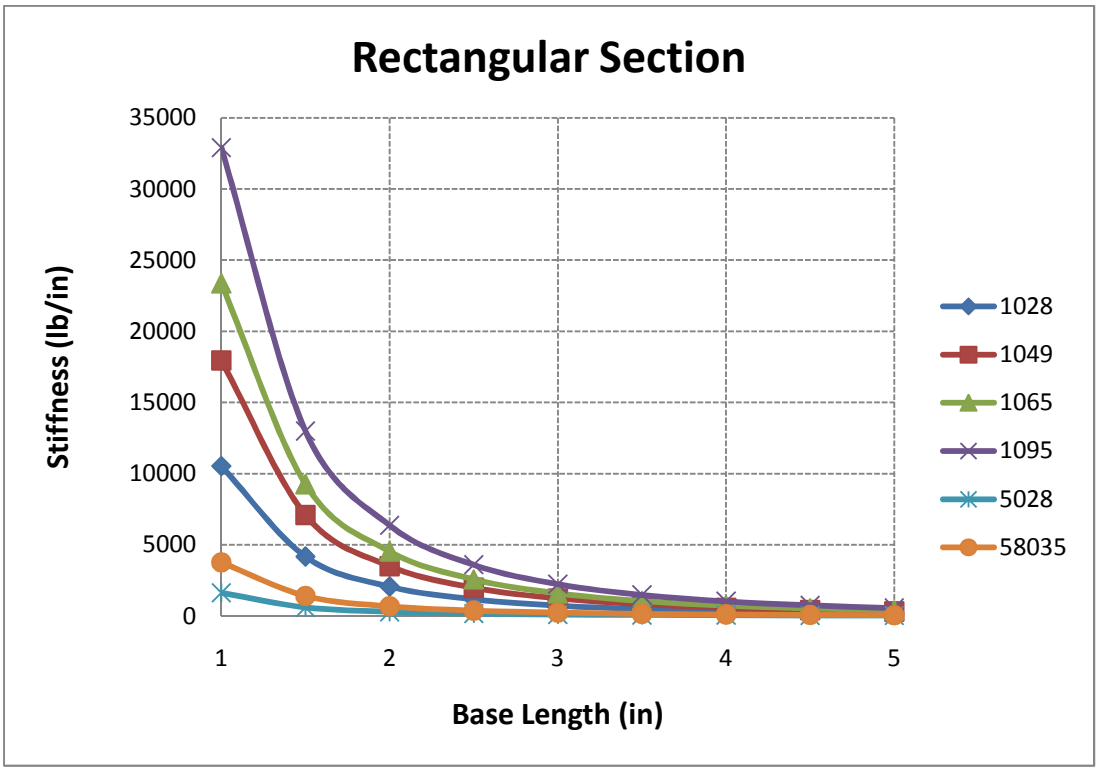

Figure 3.21 Graphical representation of linear stiffness vs. length ratio

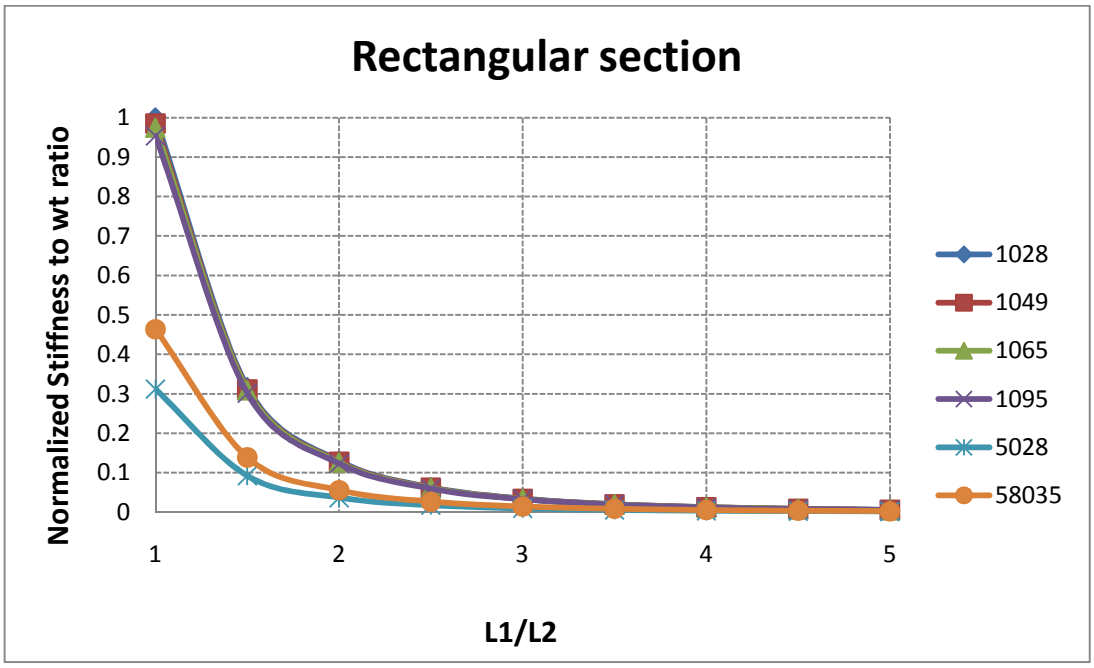

Figure 3.22 Graphical representation of normalized stiffness to weight vs. length ratio

As can be seen from the graph, for a lateral loading scenario, the thickness of the tube has negligible gain in stiffness to weight ratio whereas the OD of the tubes has a significant effect on the stiffness to weight ratio. This is similar to that of flexural stiffness as the loading is a bending moment at the end and not in the middle. Hence, the graph also depicts that for a L_1/L_2 ratio of 2 and above, the gain in stiffness to weight ratio is negligible.

3.3.4 Application (guidelines)

The analysis of various cases shown above provides a guideline for designing a structure based on its application and loading conditions. The guidelines to designing a structure are given below,

1. As the stiffness of the structure depends more on the outer diameter than the thickness, the initial constraint should be to fix the size of the outer diameter of the tube and then constrain a specific wall thickness based on the application/loading conditions.
2. Once the structure is designed with a fixed OD and a certain wall thickness, check if the stiffness of the structure meets the desired requirement i.e., max deflection.
3. Next we need to check for the stresses in the structure based on the load applied on it. The length of the tubes in bending can be estimated from the formula provided below,

$$L = fos * \frac{4}{P} * \frac{\sigma_y * I}{c}$$

Where, $I = c^2 * \frac{\pi}{4} (D_o^2 - D_i^2)$

$c = Distance\ of\ the\ outermost\ element\ from\ the\ neutral\ axis$

$P = Load\ ; L = length\ of\ the\ frame$

$fos = Factor\ of\ safety$

By increasing the thickness of the tubes, the strength of the structure also increases. But there is a limitation on the minimum thickness of the tube in order to avoid local buckling which is explained in section 3.3.5.1.

4. Also based on the application of the structure, the orientation of the tubes are to be decided. For example, race car frame requires the driver's legs to pass through the structure and hence cannot be triangulated diagonally across whereas for a tower/pyramid the diagonal triangulation is possible.
5. Hence the design of the structure is an iterative process between the OD and thickness to satisfy the given loads and the orientation of the tubes are dependent on the application.

3.3.5 Triangulation requirement study

From the results mentioned above, there is a clear need for triangulation beyond a certain L_1/L_2 ratio for each type of loading scenario. The question that arises next is how much triangulation is required to maintain or improve the stiffness to weight ratio of the design. The factors affecting the effectiveness of a triangulation member are,

3.3.5.1 Orientation of the tube – Tension / Compression

The orientation of the tube determines if the tube is going to be in tension or compression. In order for the triangulation to be effective, it should be oriented such that it is under tension. Compression loads on a thin walled member can cause it to buckle. In such a case, the tube would have to be bigger and ultimately have more weight than what is required. Hence the stiffness to weight of a triangulation is higher for a tube in tension.

In order to calculate the critical thickness to diameter ratio of a thin walled cylindrical tube to avoid local buckling, we use the following formula [13],

$$\sigma' = \frac{E}{\sqrt{3}} \frac{1}{\sqrt{1-v^2}} \frac{t}{R}$$

Where, $\sigma' = critical\ stress\ (yield)$

$E = Young's\ modulus,\ v = Poisson's\ ratio$

$t = thickness,\ R = mean\ radius\ of\ the\ tube$

According to [13], the theoretical stress obtained from this formula is 40% to 60% higher than the critical stress actually seen during testing. Hence the formula is reduced to

$$\sigma' = \frac{0.3Et}{R}$$

$$\frac{t}{R} = \frac{63100}{0.3 * 2.97 * 10^7}$$

$$\frac{t}{R} = 0.00708$$

By including a factor of safety, the rule of thumb [9] to prevent failure due to local buckling of the tube is

$$\frac{t}{D} = \frac{1}{50} = 0.02$$

The tubes used in this study meet or exceed the minimum criteria to avoid local buckling.

3.3.5.2 Constant thickness to outer diameter ratio

The ratio of thickness to outer diameter corresponds to the first rule of thumb. The OD and the thickness increase in size linearly or by the same amount, then the stiffness increases by a factor of 4 and the strength increase by a factor of 3. Since the weight also increases by a factor of 2, the overall stiffness to weight is still higher, by a factor of 2.

Let us consider the lateral bending case to demonstrate the increase in stiffness to weight of the structure by adding two different size tubes but have the same

thickness to OD ratio. The Fig 3.23 shows the braced structure along with the loads and constraints applied to the structure.

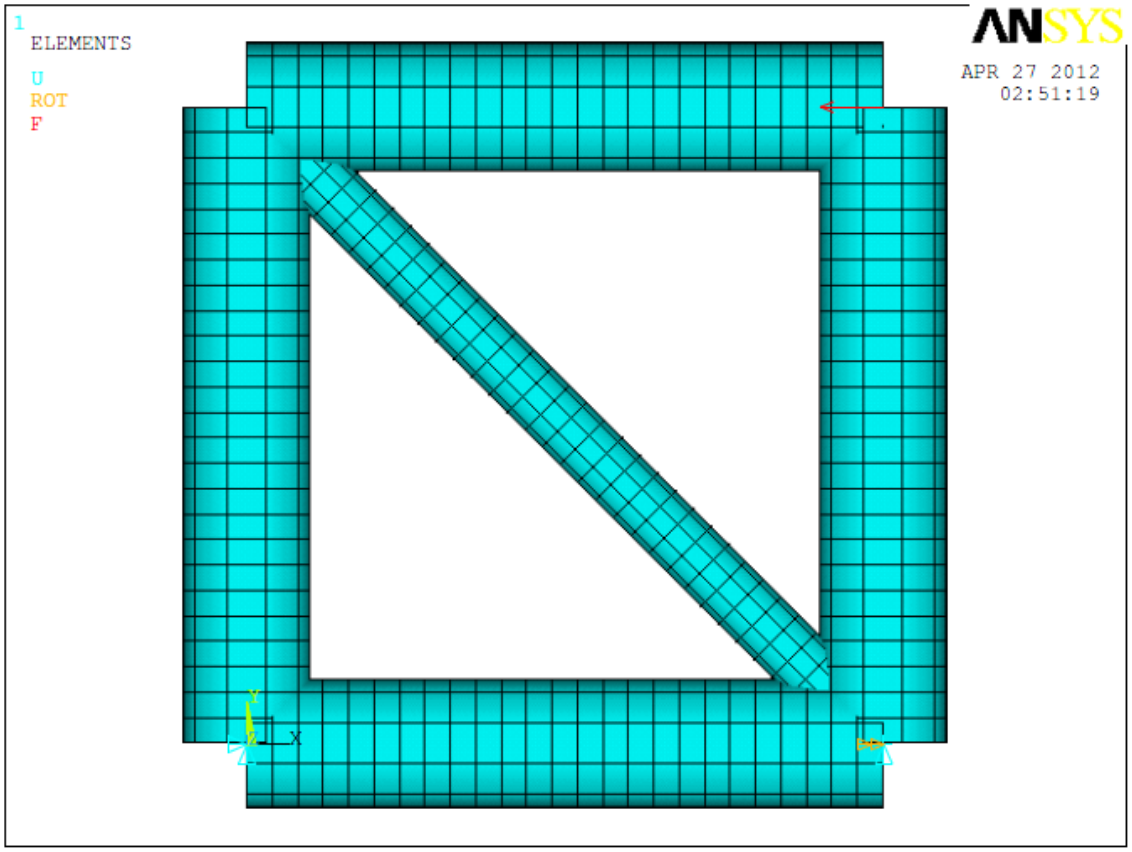

Figure 3.23 Constraints and forces for lateral bending case with bracing

In this study, a rectangular section composed of 1 inch OD and 0.028 inch thick tubes is constructed. The bracing acts in tension with the load to further decrease the chances of buckling. The structure is allowed to deform in a two dimensional place and hence 3 rigid body modes are restrained. A force of 100 N is applied at the node as shown in the figure and the resulting displacement and stresses are shown in Fig 3.24 below,

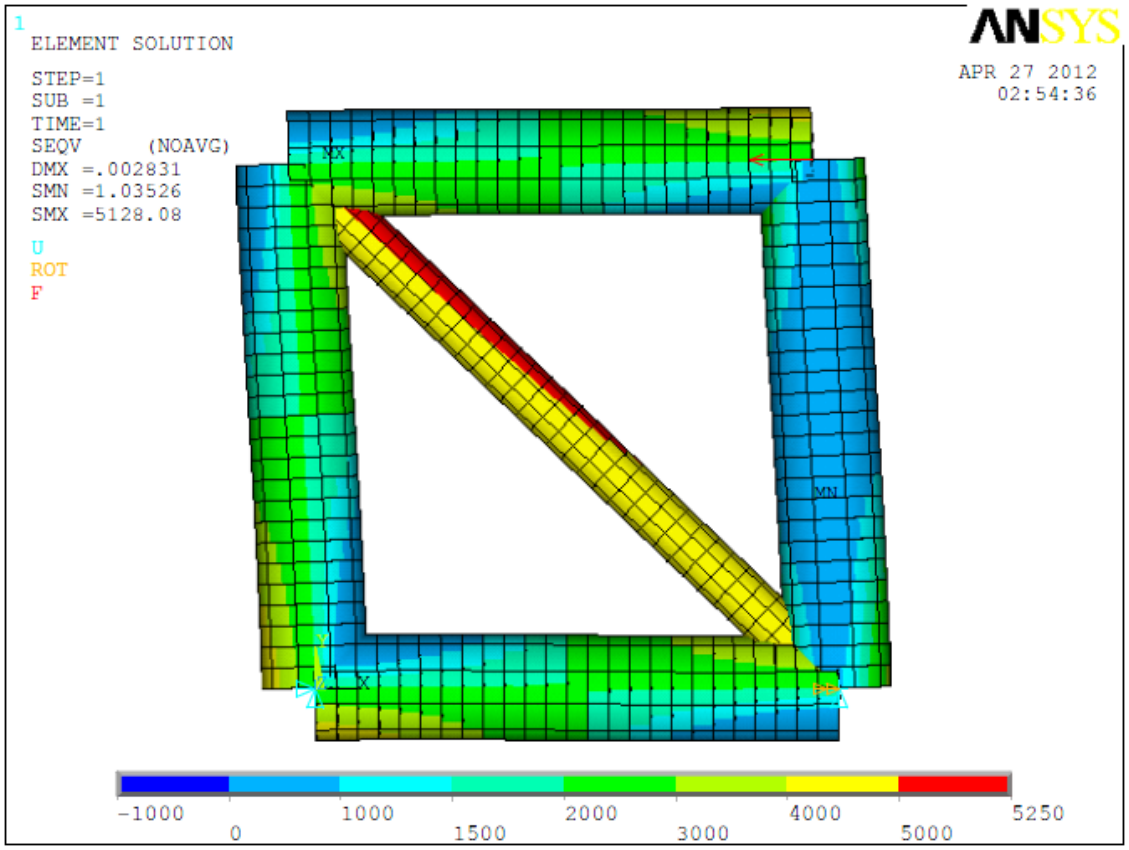

Figure 3.24 Stress distribution for lateral bending case with bracing

The analysis is repeated for varying length ratios and also different bracing tube sizes. The two sizes considered in this study are

- 5/8” OD X 0.035” thickness circular tube - 58035
- 1/2” OD X 0.028” thickness circular tube - 05028

The equivalent stiffness to weight ratios are calculated for both types of bracing and is compared to the same structure without bracing. The Fig 3.25 represents a comparison between the braced and unbraced structure.

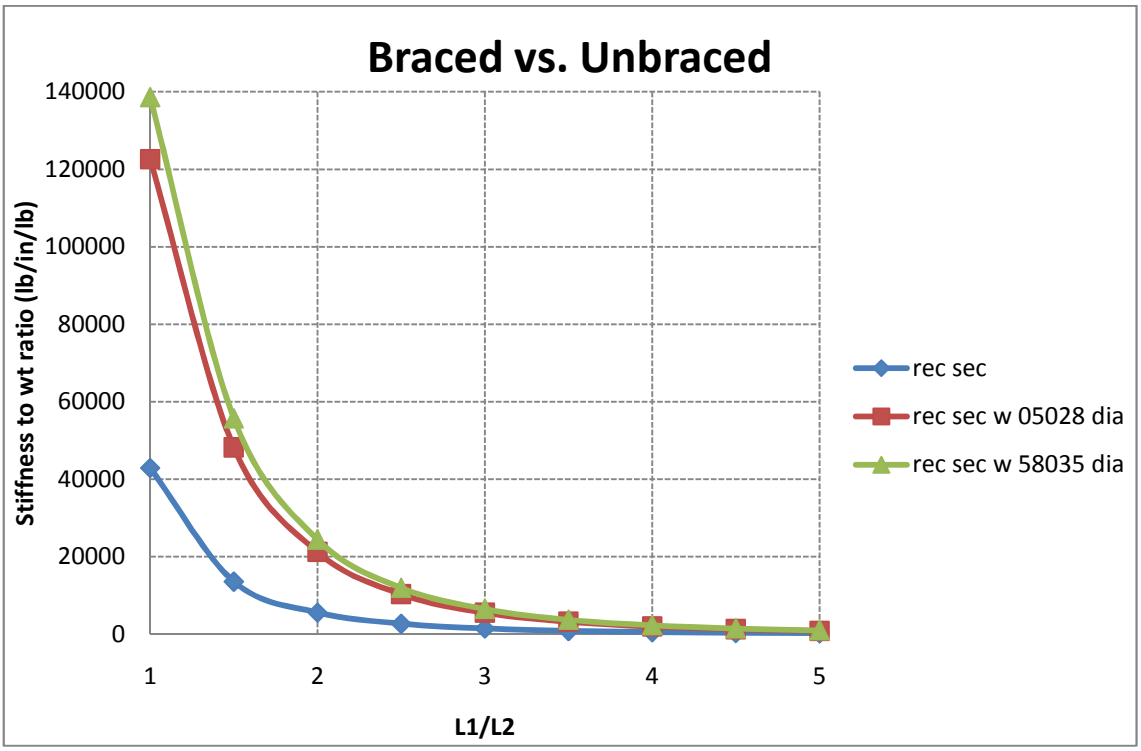

Figure 3.25 Graphical representation of braced vs. unbraced structure

The graph clearly indicates the increase in stiffness to weight ratio for a braced section as compared to an unbraced one.

3.3.5.3 Angular placement

The angular placement has a high impact on the stiffness of the structure. This factor is directly related to the ratio of the lengths of the rectangular section. The graph below shows how the angle affects stiffness to weight ratio. For a ratio of L_1/L_2 equal to 1, the angle is 45 degrees and it has the maximum stiffness as well as stiffness to weight ratio. This value further decreases as the angle gets smaller. From the graph it can observed that an angular variation from 30° to 60° has a significant effect on the stiffness to weight ratio.

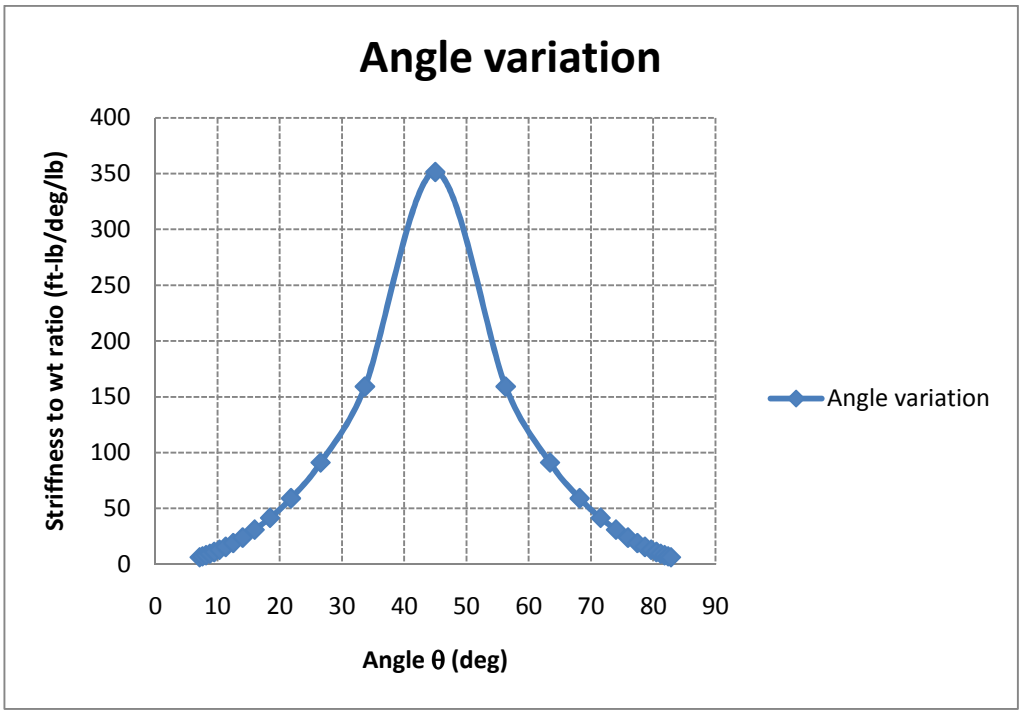

Figure 3.26 Graphical representation of angle variation

3.3.5.4 Bracing Increments

Using the result from the graph obtained above, the next step is to vary the number of triangles in a rectangular section to observe the variation in stiffness to weight ratio. The same rectangular section with a 05028 bracing is used to find the maximum number of triangles that can be formed to give the highest stiffness to weight ratio.

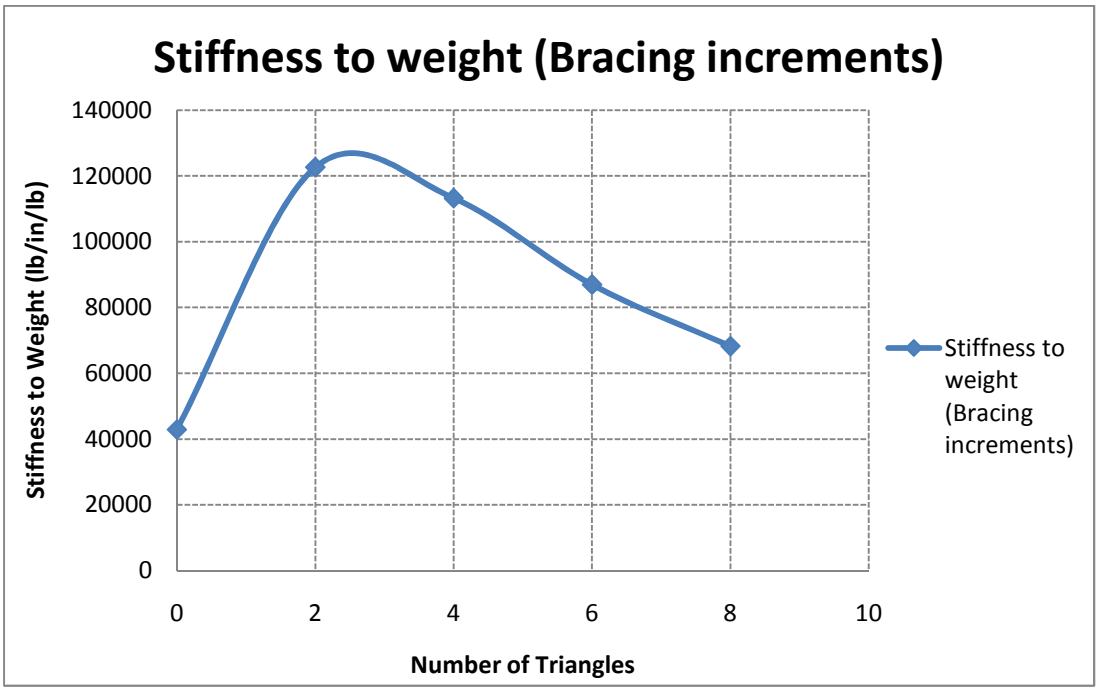

Figure 3.27 Graphical representation of bracing increments

The graph above shows that the maximum number of triangles that give the highest stiffness to weight ratio is 2. This result holds true for bracing of any size as the weight increases linearly hence giving the same result.

These are the various factors to be considered while designing a structure and their importance to stiffness to weight ratio. The next section verifies the conclusions reached by the above processes by running an iterative study of the same experiments shown above.

CHAPTER 4

DESIGN OF EXPERIMENTS USING HYPERSTUDY

4.1 Design of Experiments (DOE)

Design of experiments is a series of tests in which design variables of a process are changed in order to observe the change in the response of the process. For example, in designing a part, the design variable of its shape and size can be changed in order to study its effect on the output response. The DOE studies not only provide the effects on the response but also the interaction of each design variable with one another and see the overall change in the output. Once the DOE is complete, a regression can be obtained of all the input design variables as a function of the output. [14]

4.1.1 Steps in DOE process

The following steps are executed in order to run a DOE analysis [14],

1. Create the design variables (inputs)
2. Perform nominal run to create responses (outputs)
3. Select the DOE type (full factorial, fractional, etc) for controlled and/or uncontrolled factors.
4. Export the solver input files for the specified runs in the DOE study.
5. Solve the exported files and extract the responses.
6. Analyze the main effects plots, interaction plots and the sensitivity index.

4.1.2 Objective of DOE process

The objective of the DOE is to provide the following plots to describe the effect of design variables on the response,

1. Main effects – These plots provide information on the influence each design variable has on the response.
2. Interaction – These plots give the interdependence of each variable with one another. It provides the effect on the response while changing multiple design variables simultaneously rather than independently.

Once the DOE is generated, the various runs are extracted using statistical regression techniques to generate an approximation model. The approximation will give a linear or quadratic relation of the design variables and the required response. This generated approximation will also provide an Analysis of Variance (ANOVA) plot describing the contribution of each design variable or set of design variables on the response. [14]

4.2 Approximation

An approximation is the formulation of a mathematical expression which is used to substitute the nominal curve of the actual responses with a very high closeness to fit. This approximation model is used in order to minimize the use of computational resources for optimization studies. The drawback of using an approximation model is the tradeoff between accuracy and efficiency. This is dependent on the type of regression used in the formulation of the approximation. [14]

Regression is the polynomial expression which provides a relation between the design variables and the response. The accuracy of the regression models changes by increasing the order of the polynomial which increases the number of runs performed to obtain the

approximation. Hyperstudy uses the following three methods to generate an approximation model,

4.2.1 Least square regression

The least square regression method is used to provide a fitted line with a degree of "closeness" to the plotted points. This closeness is maintained by reducing the residuals i.e., the vertical distance of the points from the line, and keeping it small. Hence it minimizes the sum of squares of vertical deviations from the points to the line. [15]

4.2.2 Moving least square method

In this method, a continuous function is constructed for a set of points by calculating the weighted least square measure around the point. This method gives a good loacalized approximation but can lead to the generation of local minimum's which are not present in the actual response. [14]

4.2.3 Hyperkriging method

Hyperkriging provides the best prediction as it was designed for geophysical variables with a continuous distribution. This method interpolates an elevation value by calculating a weighted average of the vector points i.e., it analyzes the statistical variation in points over different distances and directions to produce the minimum error in the elevation estimate. [14]

As the focus of this thesis is to generate an approximation with the regression coefficients, the least square method is chosen. The accuracy of the approximation can be estimated using the coefficient of determination i.e., the R^2 value of the equation.

4.3 Design of Experiments (DOE) for stiffness

4.3.1 DOE for torsional stiffness

The data collected form the Ansys model is used to run the DOE. The spreadsheet is prepared by arranging the serial numbers in column 1, length (L_1) in column 2, Outer Diameter in column 3, Thickness in column 4 and the response which is the stiffness to weight ratio in column 5. The DOE is setup in Hyperstudy and is made to run using the matrix from the text file. The following results are achieved.

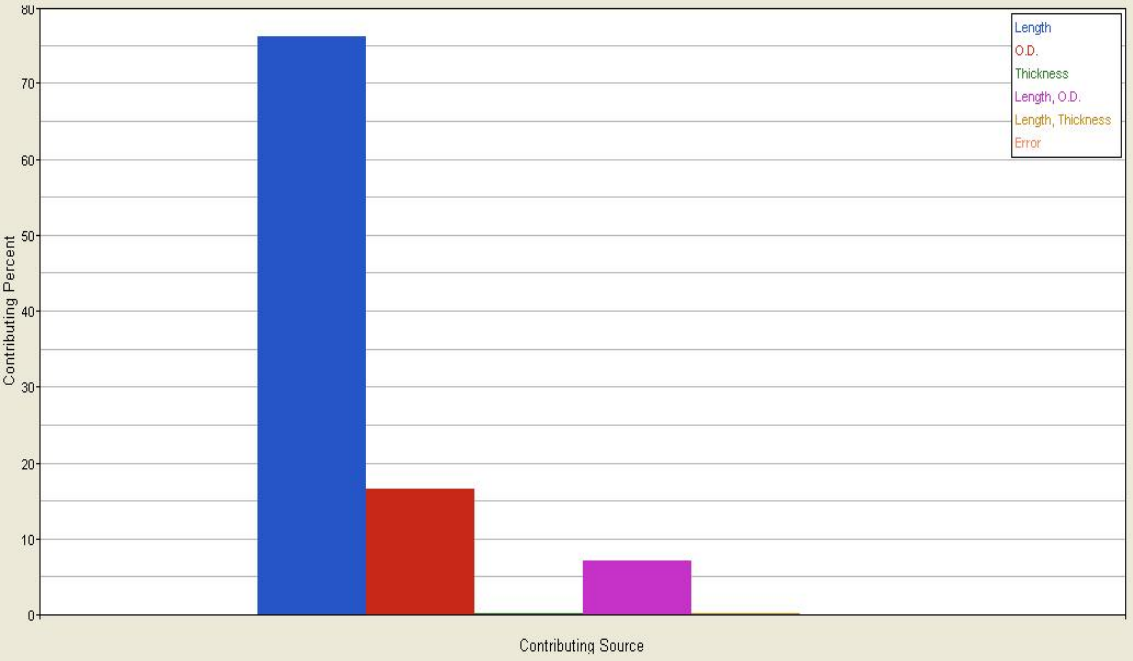

Figure 4.1 Graphical representation of ANOVA for torsional stiffness

The graph 4.1 shows an ANOVA plot which is the analysis of variance in the DOE. According to this graph, the length has the maximum effect on the stiffness to weight ratio. The OD has little effect but the thickness has negligible effect on the response.

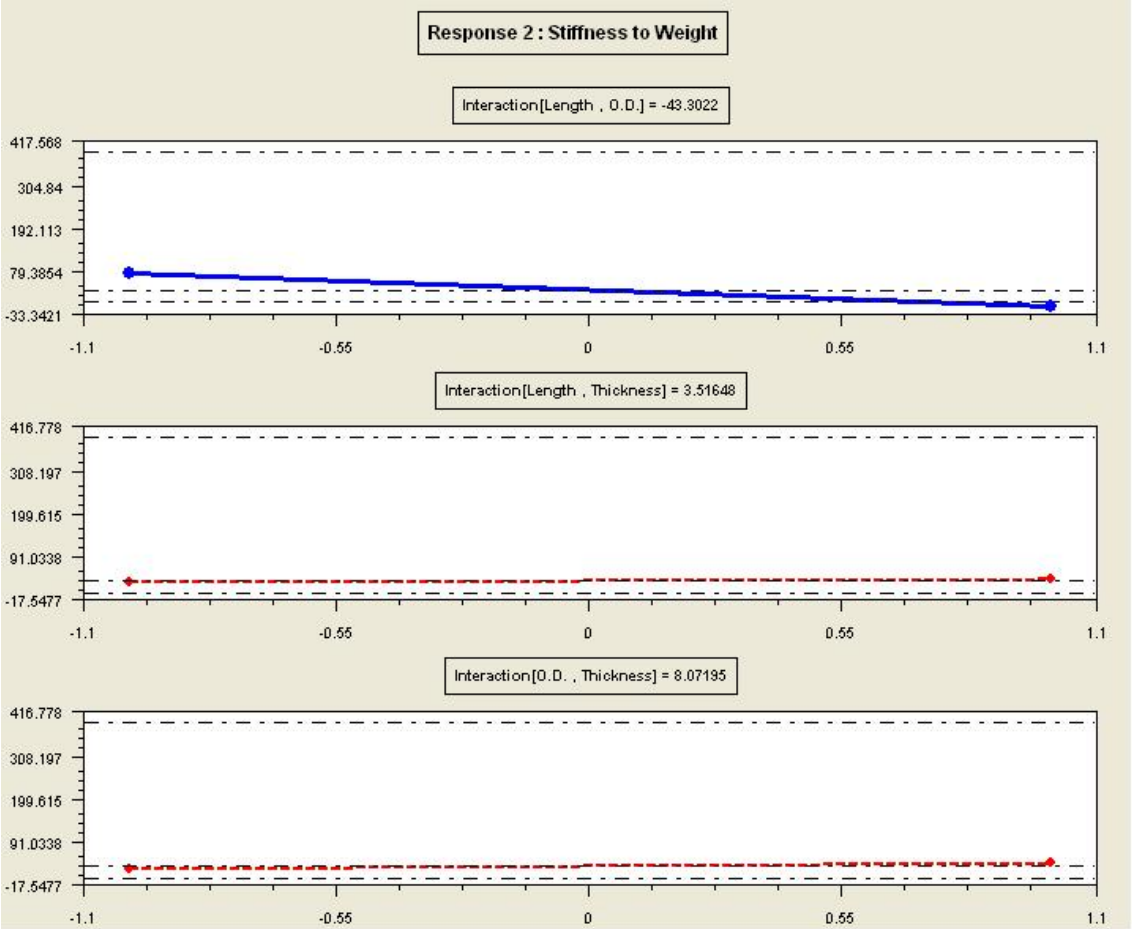

Figure 4.2 Interaction plots for torsional stiffness

The fig 4.2 and 4.3 represent the interaction and main effects plots. The interaction plots signify the amount of variance in the response due to the interaction of the two design variables where as the main effects plots display the variance in the response due to each design variable. Fig 4.2 suggests that there is high interaction between the length and OD whereas the interaction of these two design variables with thickness is small and hence neglected. Fig 4.3 depicts the main effects of the design variables on the response and hence shows that the length has a higher effect on the response and the effect of thickness is insignificant. This is determined by looking at the slope of the line in the main effects plots.

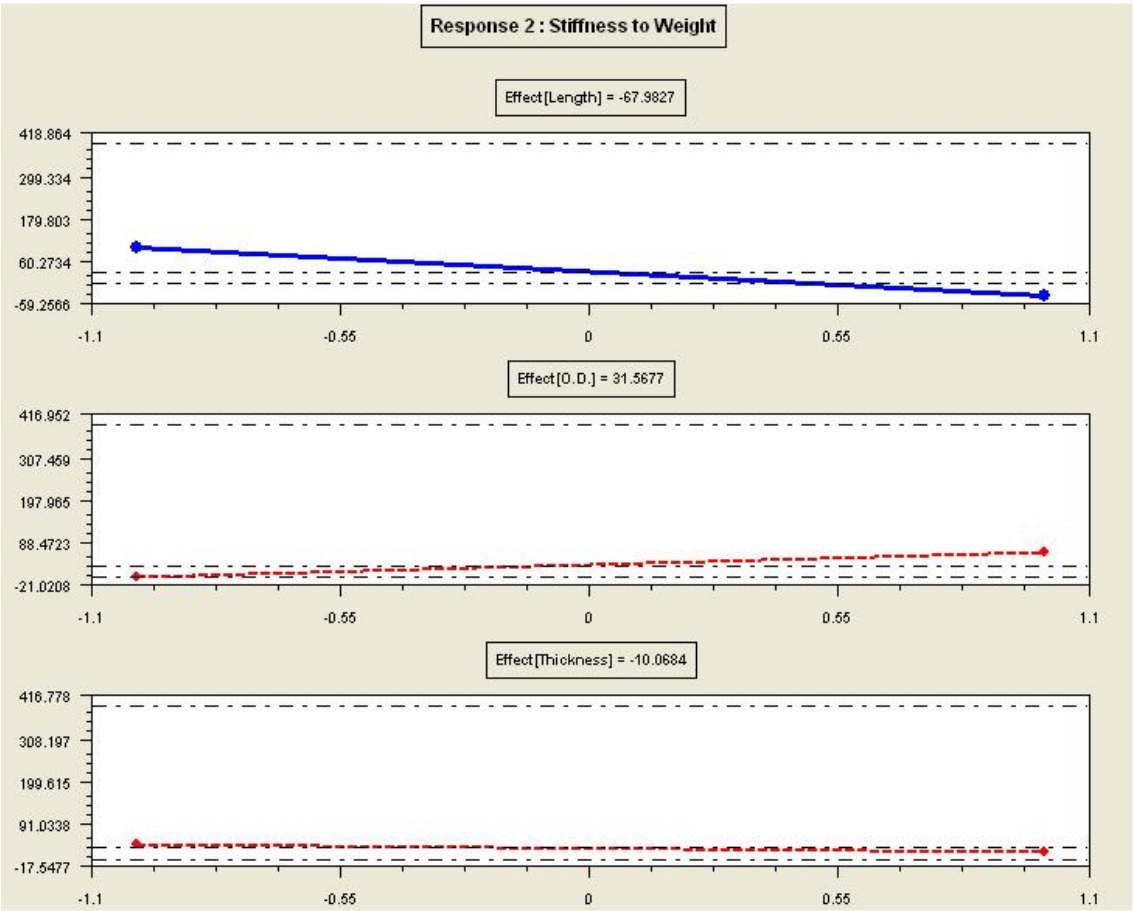

Figure 4.3 Main effects plot for torsional stiffness

The next step is to run the approximation study using the results of the DOE. A linear regression of the extracted information gives a regression equation of the design variables as a function of the response.

Regression Model

Order	3
Terms	Constant ▾ Apply
Confidence	95 % ▾

Reset

Diagnostics

R^2	0.9503641
R^2-Adj	0.9470071
Multiple R	0.9748662
Num Samples	222

Regression terms and coefficients

On	Coeff.	Regression Terms	Lower	Values	Upper	T-value
☑	a0	intercept	-195.19128	66.667558	328.52640	0.4990033
☑	a1	dv_1^1	-590.97589	-20.480332	550.01522	-0.0703624
☑	a2	dv_2^1	-460.43490	306.00326	1072.4414	0.7825372
☑	a3	dv_3^1	-1288.1947	-715.28740	-142.38015	-2.4471034
☑	a4	dv_1^2	-411.82844	1.8478311	415.52410	0.0087550
☑	a5	dv_2^2	-137.19177	360.05936	857.31050	1.4192353
☑	a6	dv_3^2	4000.3308	4951.4764	5902.6219	10.203374
☑	a7	dv_1^1 * dv_2^1	-1552.7853	-50.780176	1451.2249	-0.0662642
☑	a8	dv_1^1 * dv_3^1	-342.85377	42.925818	428.70541	0.2180898
☐	a9	dv_2^1 * dv_3^1	-	-	-	-
☑	a10	dv_1^3	-240.17827	-0.0493889	240.07949	-4.03e-04
☐	a11	dv_2^3	-	-	-	-
☑	a12	dv_3^3	-45944.677	-45452.911	-44961.145	-181.15873
☑	a13	dv_1^2 * dv_2^1	-412.94990	1.9430103	416.83592	0.0091790
☑	a14	dv_1^1 * dv_2^2	-997.35328	-20.644334	956.06461	-0.0414278
☑	a15	dv_1^2 * dv_3^1	-215.61380	-1.7439531	212.12590	-0.0159824
☑	a16	dv_1^1 * dv_3^2	7.8308292	228.82141	449.81200	2.0294528
☐	a17	dv_2^2 * dv_3^1	-	-	-	-
☐	a18	dv_2^1 * dv_3^2	-	-	-	-

Figure 4.4 Linear regression approximation for torsional stiffness

The coefficients of the linear regression equation are shown in the illustration above. The regression terms which are not selected had a very low T-value which signifies that the effect of that term on the approximation is minimal and hence does not have a significant effect on the R^2 (coefficient of determination) value.

Hence the approximation equation is as follows,

$$y = a_0 + a_1x_1 + a_2x_2 + a_3x_3 + a_4x_1^2 + a_5x_2^2 + a_6x_3^2 + a_7x_1x_2 + a_8x_1x_3 + a_{10}x_1^3 + a_{12}x_3^3 + a_{13}x_1^2x_2 + a_{14}x_2^2x_1 + a_{15}x_1^2x_3 + a_{16}x_3^2x_1$$

$$y = 66.67 - 20.48x_1 + 306x_2 - 715.28x_3 + 1.84x_1^2 + 360.06x_2^2 + 4951.5x_3^2 - 50.78x_1x_2 + 42.92x_1x_3 - 0.05x_1^3 - 45452.91x_3^3 + 1.94x_1^2x_2 - 20.64x_2^2x_1 - 1.74x_1^2x_3 + 228.82x_3^2x_1$$

Where, $y\ (response) = stiffness\ to\ weight(ft\ lb/\ deg\ per\ lb)$

$x_1, x_2, x_3\ (design\ variables) = Length\ (in), OD\ (in) and\ Thickness(in)\ respectively$

4.3.2 DOE for bending stiffness

Similarly, the above steps were carried out to perform a DOE for bending stiffness. The following results were achieved,

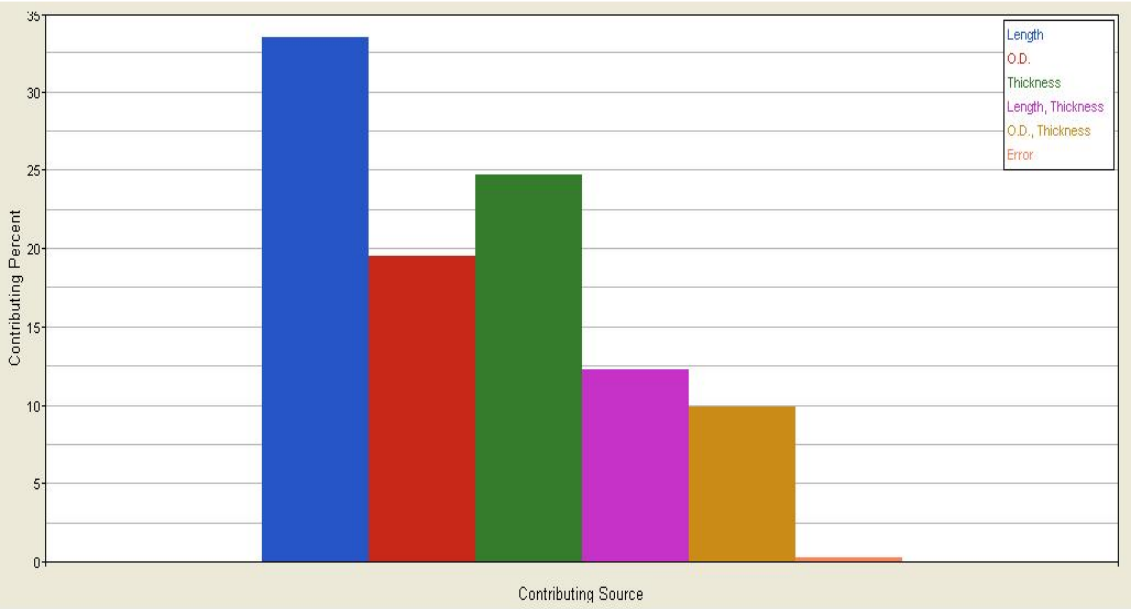

Figure 4.5 Graphical representation of ANOVA plot for bending stiffness

The graph 4.5 shows an ANOVA plot for the bending stiffness which suggests that the length has the maximum effect on the stiffness to weight ratio. The thickness of the tube is the second highest contributor to the response followed by the OD. The product of length and thickness i.e., the interaction between the two has a higher contribution than the interaction between the OD and thickness. Hence we can conclude the relevance of the design variables with respect to the response.

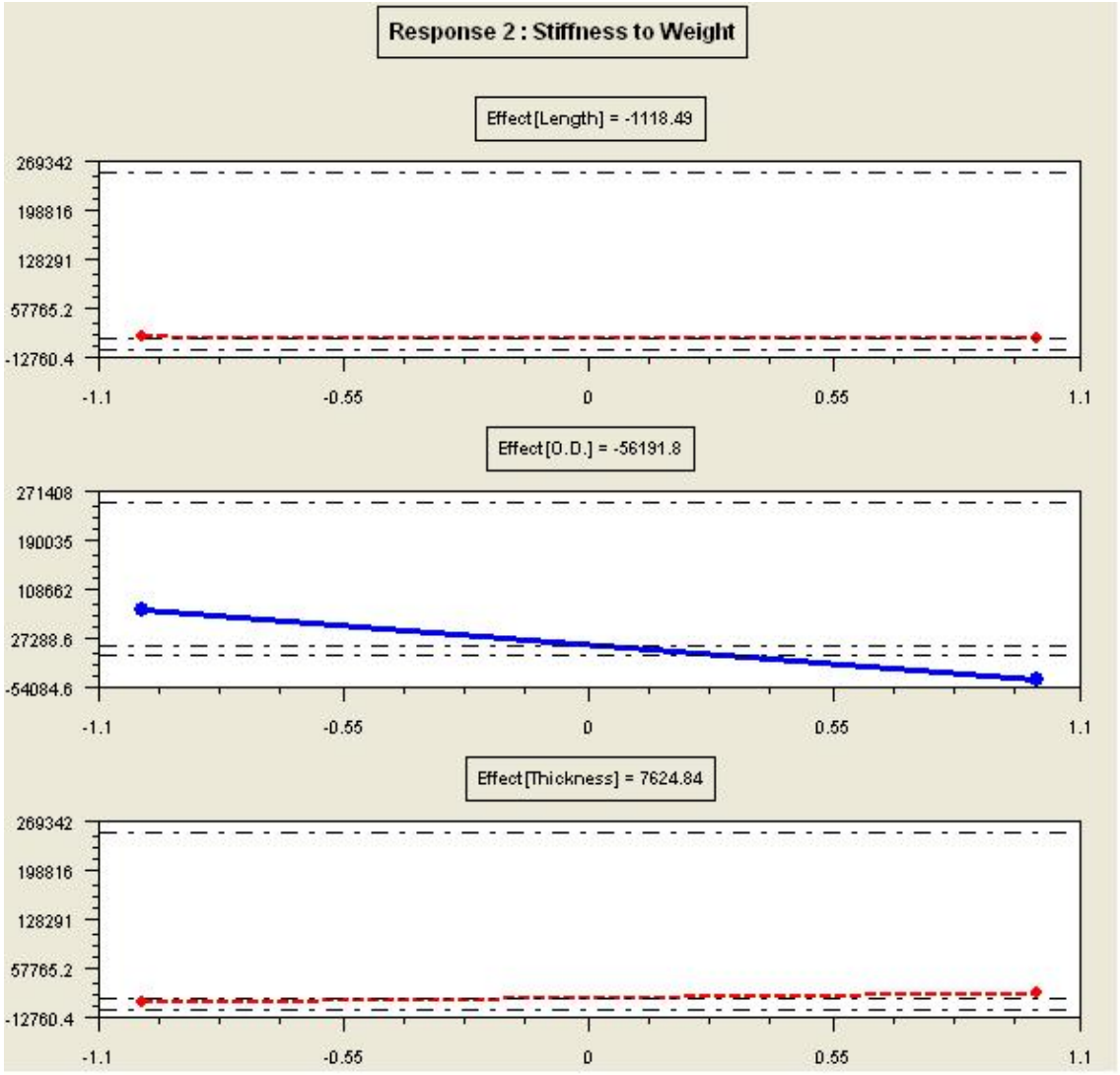

Figure 4.6 Main effects plot for bending stiffness

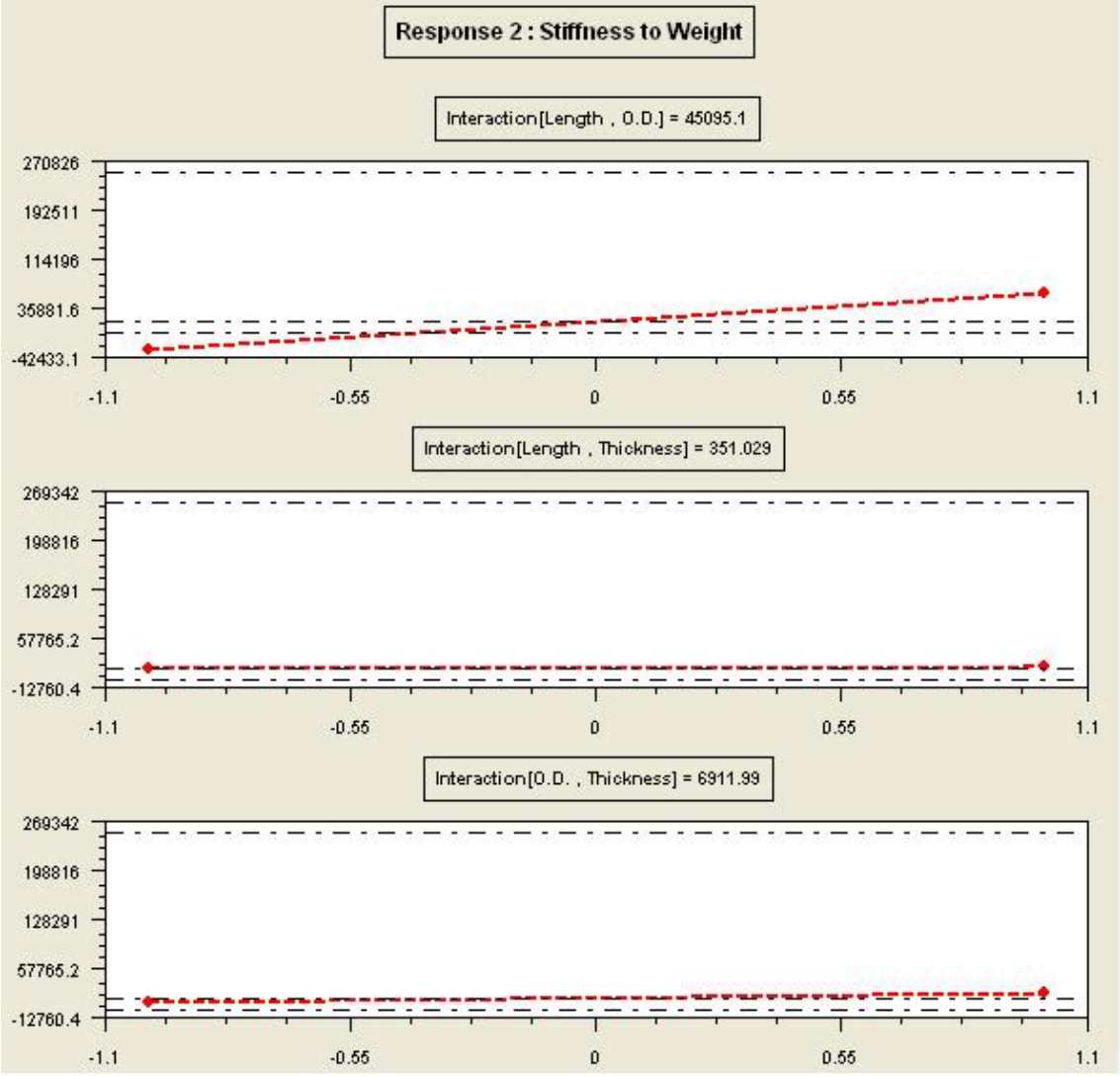

Figure 4.7 Interaction plots for bending stiffness

The fig 4.6 and 4.7 represent the main effects and interaction plots. The next step is to run the approximation study using the results of the DOE. The approximation model is as follows,

Regression Model

Order	3
Terms	Constant ▼ Apply
Confidence	95 % ▼

Reset

Diagnostics

R^2	0.8501154
R^2-Adj	0.8327734
Multiple R	0.9220170
Num Samples	136

Regression terms and coefficients

On	Coeff.	Regression Terms	Lower	Values	Upper	T-value
☑	a0	intercept	202003.70	247769.80	293535.91	10.611103
☑	a1	dv_1^1	-331894.44	-31561.620	268771.20	-0.2059741
☑	a2	dv_2^1	-1236169.4	96744.438	1429658.2	0.1422591
☑	a3	dv_3^1	-780978.44	-288433.65	204111.13	-1.1477737
☑	a4	dv_1^2	-666253.50	879.35908	668012.22	0.0025835
☑	a5	dv_2^2	-980890.75	2250.3152	985391.39	0.0044863
☑	a6	dv_3^2	651419.04	1773136.7	2894854.5	3.0982376
☐	a7	dv_1^1 * dv_2^1	-	-	-	-
☑	a8	dv_1^1 * dv_3^1	-1116506.9	34834.200	1186175.3	0.0593004
☑	a9	dv_2^1 * dv_3^1	-4222909.8	-386508.33	3449893.1	-0.1974653
☑	a10	dv_1^3	-487002.59	-7.7865367	486987.02	-3.13e-05
☑	a11	dv_2^3	-588466.37	-27.562153	588411.24	-9.18e-05
☑	a12	dv_3^3	-2219215.4	-1231025.7	-242836.00	-2.4416470
☐	a13	dv_1^2 * dv_2^1	-	-	-	-
☐	a14	dv_1^1 * dv_2^2	-	-	-	-
☑	a15	dv_1^2 * dv_3^1	-349825.11	-342.01189	349141.08	-0.0019181
☑	a16	dv_1^1 * dv_3^2	-1000096.6	-13340.576	973415.46	-0.0264985
☐	a17	dv_2^2 * dv_3^1	-	-	-	-
☑	a18	dv_2^1 * dv_3^2	-2216630.7	232123.93	2680878.5	0.1857936

Figure 4.8 Linear regression approximation for bending stiffness

In the case of bending stiffness, the best R^2 value that could be achieved was 0.85 as the residuals in this case were higher than in the torsional case. A higher order i.e., order 4, improves the accuracy of the approximation but increases the number of runs to achieve the model. The accuracy of the approximation was improved by removing some of the outliers which are the residuals not present within the x and y limits of the approximation. These residuals are caused due to non-linearity in the data as a result of expanding the range or limits.

4.4 Design of Experiments for Stresses (Bending)

The spreadsheet is populated with the required design variables and their equivalent responses as shown in Fig 4.9. The spreadsheet is referenced to the DOE study in Hyperstudy.

	A	B	C
1	**Bending DOE**		
2			
3	**Design Variables**		
4	Load(lb) - P	200	
5	Height(in) - L2	5	
6	O.D.(in)	1	
7	Thickness (in)	0.028	
8			
9	**Responses**		
10	Area Moment of Inertia(in^4) - I	0.271041	
11	Yield Moment(lb in) - My	6841.072	
12	Max Length (in) - L1	136.8214	
13			
14			

Figure 4.9 Spreadsheet used for the DOE

The design variables and the responses are selected accordingly from the spreadsheet. The design variables and also given upper and lower bounds in order to run the various samples for a full factorial analysis of the data. The extracted values from the DOE are displayed using the main effects plots and the interaction plots as shown in the figures below,

(a)

(b)

Figure 4.10 Main effects plots for (a) Max length w.r.t design variables and (b) Yield moment w.r.t design variables

The main effects plots suggest that the load and height of the structure have a higher contribution as compared to the OD and thickness based on the slope of the lines from Fig 4.10(a). Fig 4.10 (b) suggests that the height i.e., the distance from the neutral axis has a higher effect on the yield moment as compared to the other design variables.

The interaction plots are plotted between the response and a specific design variable while keeping another design variable constant. The response is varied for the upper and lower limit of the two design variables. The following figures show the interaction of the various design variables,

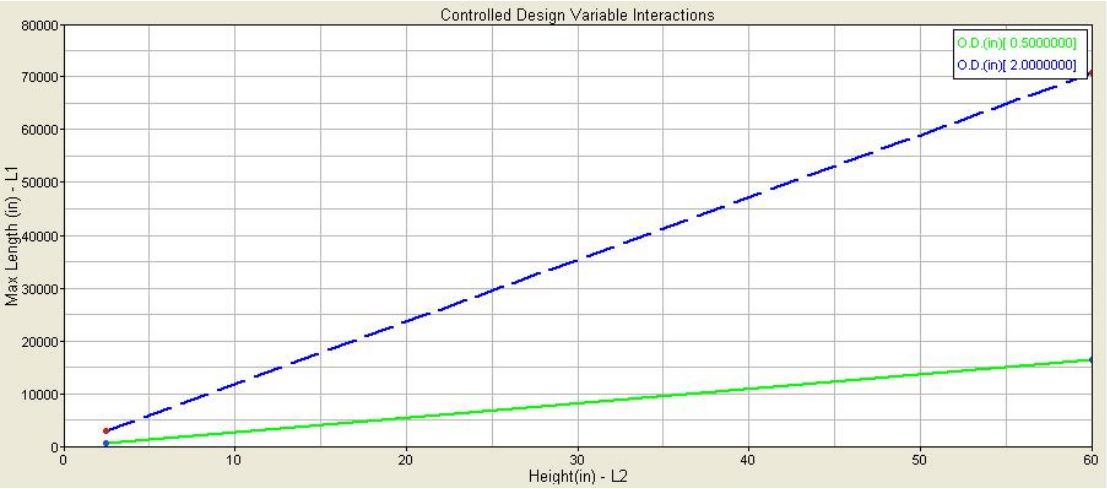

(a)

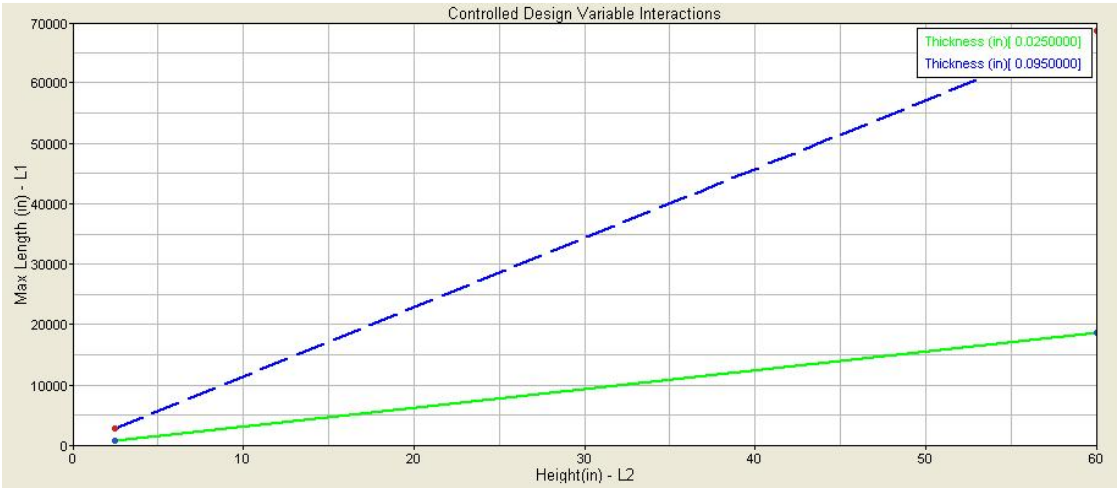

(b)

Figure 4.11 Interaction plots for Max length w.r.t. (a) height while OD is constant (b) height while thickness is constant

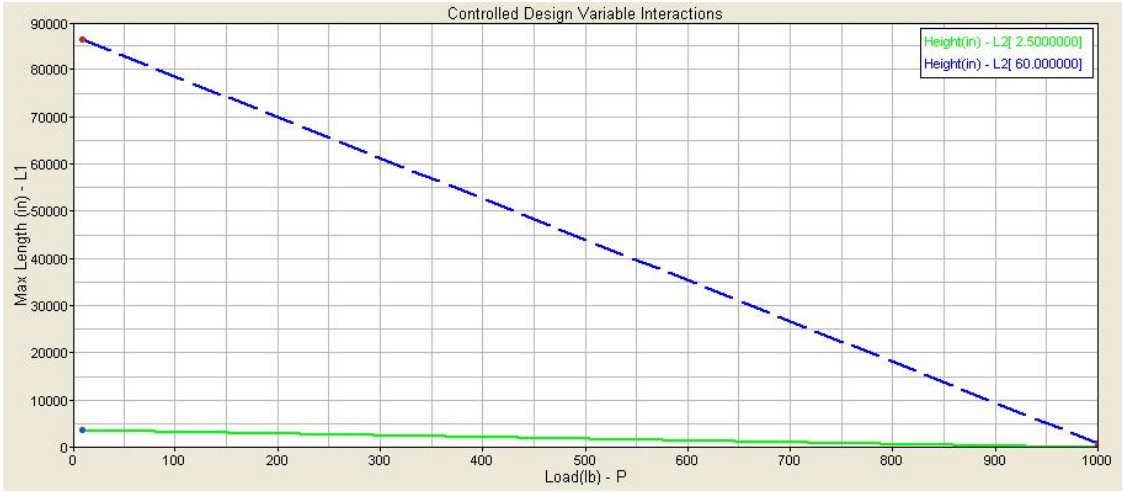

Figure 4.12 Interaction plots for Max length w.r.t. load while height is constant

Figure 4.11 plot (a) suggests that there is quite a bit of interaction between the height and the OD as the distribution is not parallel and the max length varies from approximately 3000 to 70000 when the upper limit of OD is held constant. Similarly plot (b) also shows a similar interaction between height and thickness. Figure 4.12 shows a decrease in the max length with respect to the load for a constant height.

The following interaction plots are with respect to the yield moment as a response.

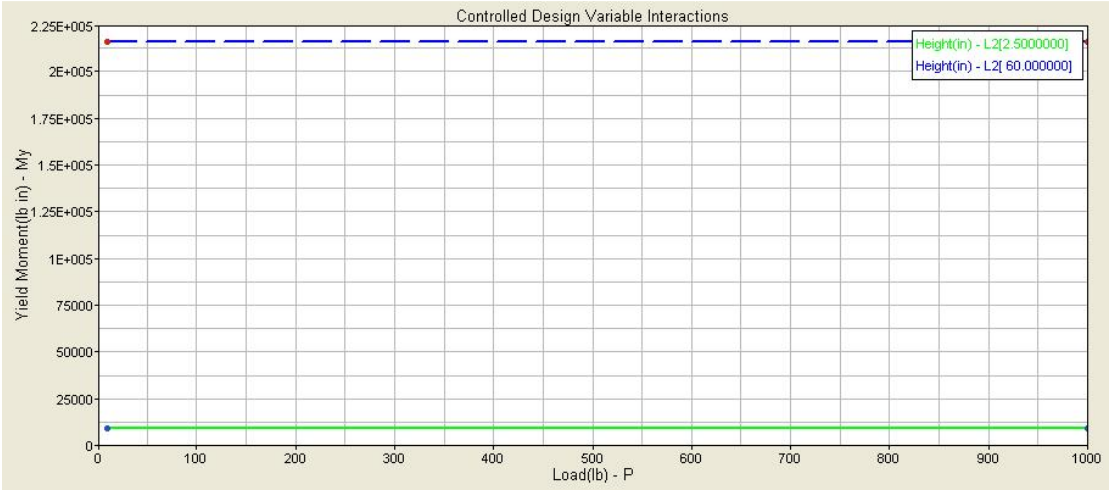

Figure 4.13 Interaction plots for yield moment w.r.t. load while height is constant

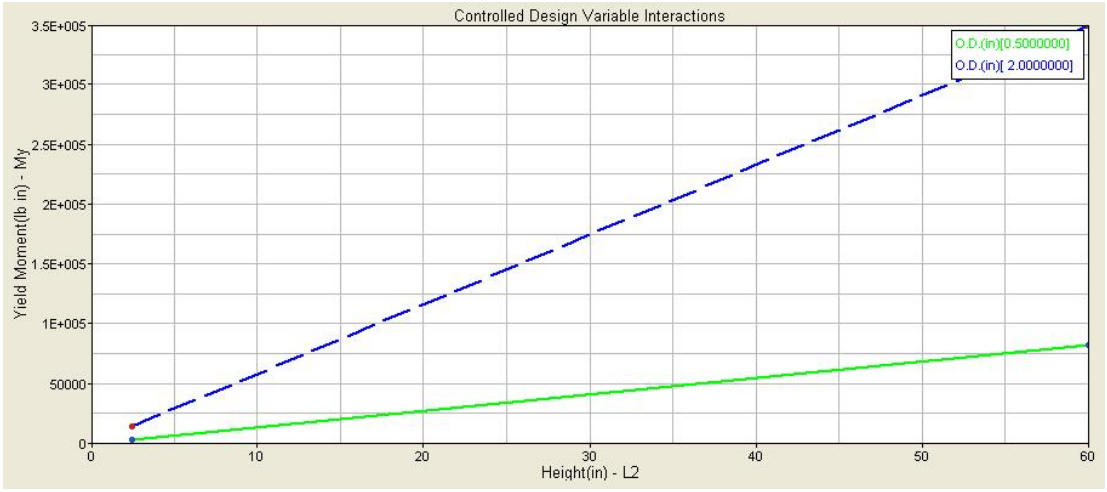

(a)

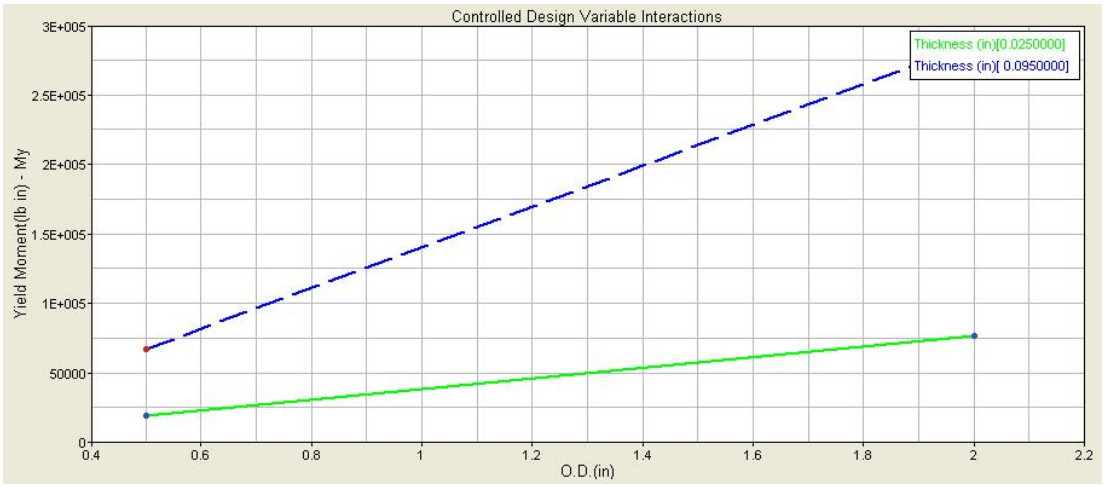

(b)

Figure 4.14 Interaction plots for yield moment w.r.t. (a) height while OD is constant (b) OD while thickness is constant

Figure 4.13 depicts that there is no interaction between the design variables as the lines are parallel to each other whereas Figure 4.14 plot (a) and plot (b) have significant interaction to affect the response.

The next step is to form the approximation for these responses with respect to each design variable. Hence the linear regression model can be developed for the variance allotted.

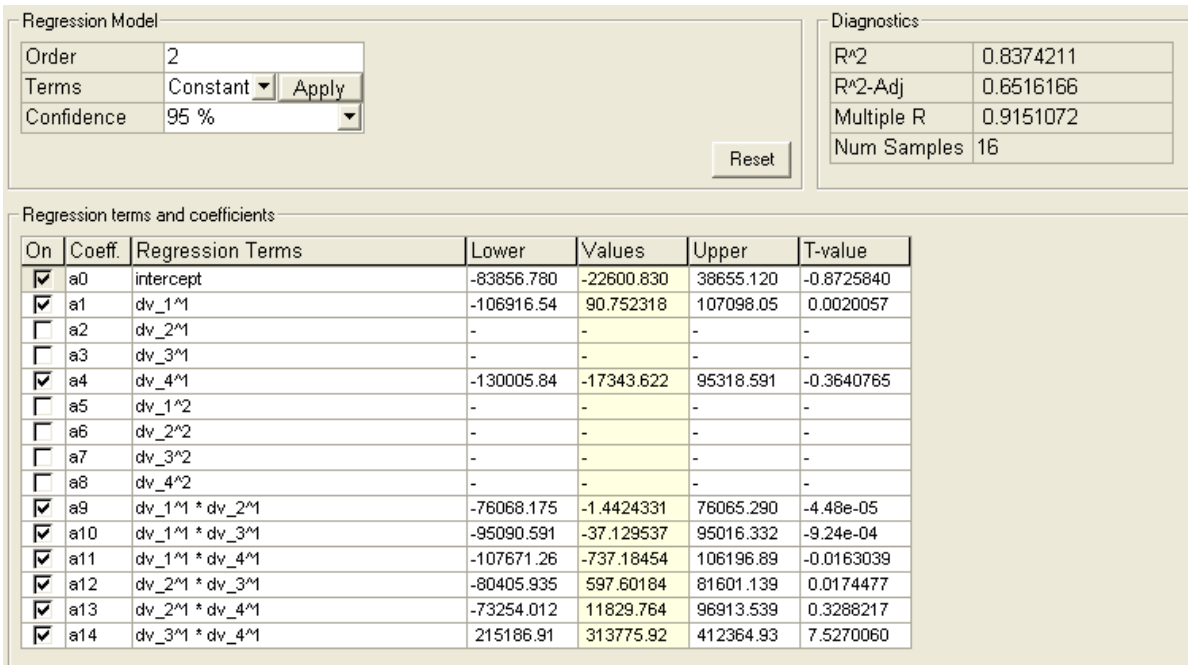

Regression Model

Order	2
Terms	Constant ▼ Apply
Confidence	95 % ▼

Reset

Diagnostics

R^2	0.8374211
R^2-Adj	0.6516166
Multiple R	0.9151072
Num Samples	16

Regression terms and coefficients

On	Coeff.	Regression Terms	Lower	Values	Upper	T-value
☑	a0	intercept	-83856.780	-22600.830	38655.120	-0.8725840
☑	a1	dv_1^1	-106916.54	90.752318	107098.05	0.0020057
☐	a2	dv_2^1	-	-	-	-
☐	a3	dv_3^1	-	-	-	-
☑	a4	dv_4^1	-130005.84	-17343.622	95318.591	-0.3640765
☐	a5	dv_1^2	-	-	-	-
☐	a6	dv_2^2	-	-	-	-
☐	a7	dv_3^2	-	-	-	-
☐	a8	dv_4^2	-	-	-	-
☑	a9	dv_1^1 * dv_2^1	-76068.175	-1.4424331	76065.290	-4.48e-05
☑	a10	dv_1^1 * dv_3^1	-95090.591	-37.129537	95016.332	-9.24e-04
☑	a11	dv_1^1 * dv_4^1	-107671.26	-737.18454	106196.89	-0.0163039
☑	a12	dv_2^1 * dv_3^1	-80405.935	597.60184	81601.139	0.0174477
☑	a13	dv_2^1 * dv_4^1	-73254.012	11829.764	96913.539	0.3288217
☑	a14	dv_3^1 * dv_4^1	215186.91	313775.92	412364.93	7.5270060

(a)

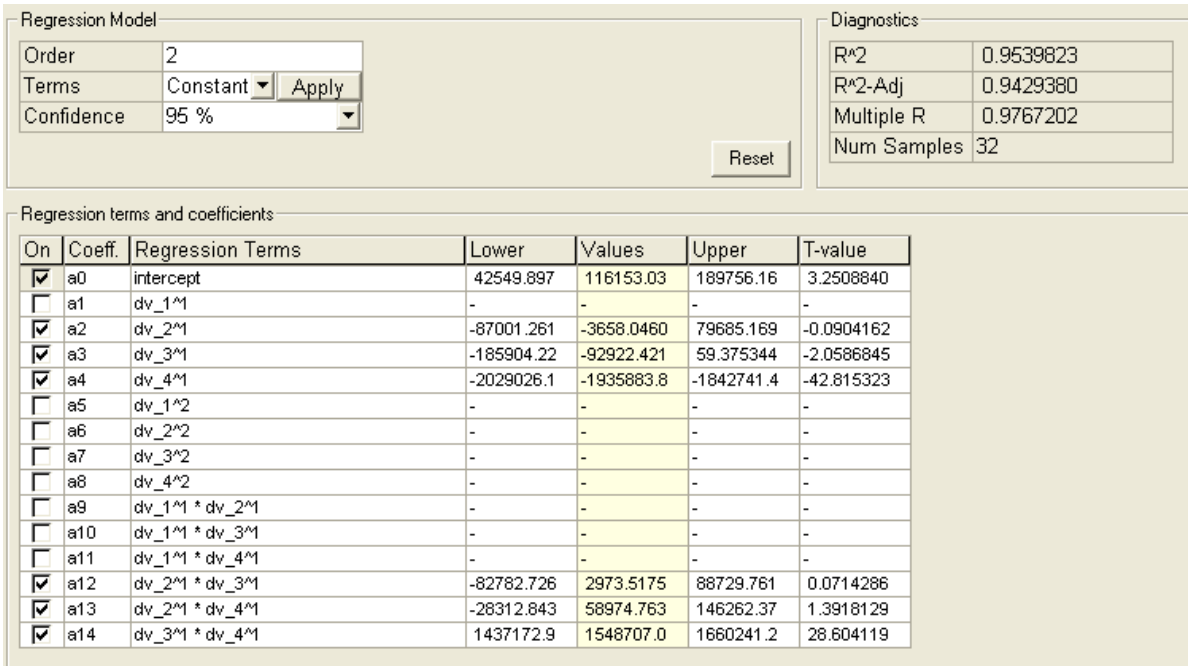

Regression Model

Order	2
Terms	Constant ▼ Apply
Confidence	95 % ▼

Reset

Diagnostics

R^2	0.9539823
R^2-Adj	0.9429380
Multiple R	0.9767202
Num Samples	32

Regression terms and coefficients

On	Coeff.	Regression Terms	Lower	Values	Upper	T-value
☑	a0	intercept	42549.897	116153.03	189756.16	3.2508840
☐	a1	dv_1^1	-	-	-	-
☑	a2	dv_2^1	-87001.261	-3658.0460	79685.169	-0.0904162
☑	a3	dv_3^1	-185904.22	-92922.421	59.375344	-2.0586845
☑	a4	dv_4^1	-2029026.1	-1935883.8	-1842741.4	-42.815323
☐	a5	dv_1^2	-	-	-	-
☐	a6	dv_2^2	-	-	-	-
☐	a7	dv_3^2	-	-	-	-
☐	a8	dv_4^2	-	-	-	-
☐	a9	dv_1^1 * dv_2^1	-	-	-	-
☐	a10	dv_1^1 * dv_3^1	-	-	-	-
☐	a11	dv_1^1 * dv_4^1	-	-	-	-
☑	a12	dv_2^1 * dv_3^1	-82782.726	2973.5175	88729.761	0.0714286
☑	a13	dv_2^1 * dv_4^1	-28312.843	58974.763	146262.37	1.3918129
☑	a14	dv_3^1 * dv_4^1	1437172.9	1548707.0	1660241.2	28.604119

(b)

Figure 4.15 Regression approximation for (a) Max length (L_1) and (b) Yield moment (M_y)

The regression terms in both approximations can be eliminated by removing the terms with insignificant T-value. These approximations hold true for the upper and lower bounds defined for the design variables. By eliminating the outliers which are generally caused by uncontrolled responses to a certain range of design variable interactions, the accuracy of the approximation can be improved.

CHAPTER 5

CONCLUSIONS AND FUTURE WORK

5.1 Conclusions

By evaluating the various loading conditions on a simplified cross-section of tubes, a trend of the design variables with respect to the responses emerge which provide information on the effect of the afore mentioned variables. The approximate models generated by the DOE provide a linear relation between the design variables and responses.

This approximation is valid only for values within the upper and lower limit described in the DOE. The accuracy of the approximation decreases as the range of variance increases. This is because the upper bound tends to increase the stresses beyond the yield strength of the material and thus causes the generation of outliers in the approximation.

The following conclusions can be drawn from this thesis,

1) The thickness of a tube for a fixed OD has negligible effect on the stiffness to weight ratio. The stiffness is a function of the moment of inertia of the c/s about the neutral axis and the stress is a function of the section modulus of the c/s, which the ratio of the moment of inertia to the distance from the neutral axis.
2) For a torsional case, the stiffness to weight ratio of a rectangular frame decreases with an increase in the ratio of the length of its sides L_1 and L_2, where L_1 is the moment arm, and the change in stiffness to weight is negligible for a L_1/L_2 ratio greater than approximately 3. Hence for a rectangular section with a L_1/L_2 ratio greater than 3, triangulation will be required.

From the fig 3.10, the increase in the stresses for a given size of tube with respect to the length ratio is small.

3) For a bending case, the stiffness to weight ratio of a rectangular frame also decreases with an increase in the ratio of the length of its sides L_1 and L_2 and the change in stiffness to weight is negligible for a L_1/L_2 ratio greater than approximately 2. Similarly for a rectangular section with a L_1/L_2 ratio greater than 2, triangulation will be required.

   From the fig 3.17, the increase in the stresses for a given size of tube with respect to the length ratio is large and maximum length for a rectangular box made of a certain tube size can be calculated from the following formula,

$$L = fos * \frac{4}{P} * \frac{\sigma_y * I}{c}$$

   Where, $I = c^2 * \frac{\pi}{4} (D_o^2 - D_i^2) (in^4)$

$$c = Distance\ of\ the\ outermost\ element\ from\ the\ neutral\ axis(in)$$

$$P = Load\ (lb); L = length\ of\ the\ frame(in)$$

$$\sigma_y = yield\ stress(psi), fos = Factor\ of\ safety$$

4) The angle variation of 30° to 60° considerably affects the stiffness to weight ratio of the structure. This indicates that the maximum number of triangles that can be created by keeping the angular variation between these limits would contribute positively to the stiffness to weight ratio of the structure.

5) The maximum number of triangles to achieve the highest stiffness to weight ratio for bracing a rectangular section is 2.

6) The stiffness to weight ratio increases for a uniform increase in OD and thickness of the tube i.e., the thickness to OD ratio remains constant.

7) From the DOE analysis, the length or the length ratio has the highest effect on the stiffness to weight ratio as compared to OD and thickness for a torsional case and the approximation is given by,

$$y = 66.67 - 20.48x_1 + 306x_2 - 715.28x_3 + 1.84x_1^2 + 360.06x_2^2 + 4951.5x_3^2 - 50.78x_1x_2 + 42.92x_1x_3 - 0.05x_1^3 - 45452.91x_3^3 + 1.94x_1^2x_2 - 20.64x_2^2x_1 - 1.74x_1^2x_3 + 228.82x_3^2x_1$$

Where, $y\ (response) = stiffness\ to\ weight(ft\ lb/\ deg\ per\ lb)$

$x_1, x_2, x_3\ (design\ variables) = Length\ (in), OD\ (in) and\ Thickness(in)\ respectively$

8) For a bending case, the length ratio and the thickness are high contributors to the response and the approximation is given by,

$$y = 247769.8 - 31561.62x_1 + 96744.5x_2 - 288433.6x_3 + 879.4x_1^2 + 2250.3x_2^2 + 1773136.7x_3^2 + 34834.2x_2x_3 - 386508.4x_1x_3 - 7.78x_1^3 - 27.56x_2^3 - 1231025.7x_3^3 - 342x_1^2x_3 - 13340.57x_3^2x_1 + 232124x_3^2x_2$$

Where, $y\ (response) = stiffness\ to\ weight(ft\ lb/\ deg\ per\ lb)$

$x_1, x_2, x_3\ (design\ variables) = Length\ (in), OD\ (in) and\ Thickness(in)\ respectively$

5.2 Future work

The suggested topics for further study are,

1) Increasing the range of variance for the design variables and obtaining a higher R-squared value.
2) Application of more advanced statistics like D-Optimal, Box Behnken, etc to improve accuracy.
3) Physical bench testing in order to create a stochastic study of the design vaiables.
4) Performing the same study using different material such as aluminum and carbon fiber.

APPENDIX A

SAMPLE ANSYS CODES FOR TORSIONAL TESTING OF RECTANGULAR STRUCTURE

```
KEYW,PR_STRUC,1          !Selecting structural menu (preferences)
KEYW,PR_THERM,0
KEYW,PR_FLUID,0
KEYW,PR_ELMAG,0
KEYW,MAGNOD,0
KEYW,MAGEDG,0
KEYW,MAGHFE,0
KEYW,MAGELC,0
KEYW,PR_MULTI,0
KEYW,PR_CFD,0

/prep7

ET,1,BEAM188             !Beam Type

MPTEMP,,,,,,,,           !Material Property
MPTEMP,1,0
MPDATA,EX,1,,2.97e7      !Modulus of Elasticity
MPDATA,PRXY,1,,.29       !Poisson's Ratio (.29)


SECTYPE, 1, BEAM, CTUBE, , 0   !Beam Section Type
SECOFFSET, CENT
SECDATA,.472,.5,10,0,0,0,0,0,0,0

k,1,0,0,0,,,,            !Creating keypoints
k,2,5,0,0,,,,
k,3,5,5,0,,,,
k,4,0,5,0,,,,

l,1,2                    !Creating line elements
l,2,3
l,3,4
l,4,1


FLST,5,12,4,ORDE,2       !Meshing the lines with the circular cross section
FITEM,5,1
FITEM,5,-12
CM,_Y,LINE
LSEL, , , ,P51X
CM,_Y1,LINE
CMSEL,,_Y
LESIZE,_Y1,.2, , , , , ,1   !Mesh every .20 inches
FLST,2,12,4,ORDE,2
FITEM,2,1
```

```
FITEM,2,-12
LMESH,P51X

/eshape,1

/GO                                  !Applying constraints
DK,4, ,0, ,0,UX,UY,UZ, , , ,
FLST,2,1,3,ORDE,1
FITEM,2,4
!*
/GO
DK,1, ,0, ,0,UX,UZ, , , , ,
FLST,2,1,3,ORDE,1
FITEM,2,2
!*
/GO
DK,3, ,0, ,0,UZ, , , , , ,
FLST,2,1,3,ORDE,1
FITEM,2,3
!*
/GO                                  !Applying loads
FK,2,FZ,100
FINISH
/SOL
! /STATUS,SOLU
SOLVE
FINISH

/post1                               !Postprocessing

PRRSOL                               !List all Nodal Reactions
PLESOL, S,EQV, 0,1.0                 !Von Mises Stress Plot
```

REFERENCES

1. Costin, M., Phipps, D., 1961, *Racing and Sports Car Chassis Design*, B.T.Batsford Ltd, London, pp. 1-16

2. Wan, M., 1998, " Different Types of Chassis," *AutoZine Technical School*, http://www.autozine.org/technical_school/chassis/tech_chassis.htm

3. Chen, W., Lui, E.M., 2005, *Handbook of Structural Engineering*-2nd edition, CRC Press.

4. Gartner, M., 1999, "Chassis Design Tips", http://www.gmecca.com/byorc/dtipschassis.html

5. Riley, W.B., George, A.R., 2002, "Design, Analysis and Testing of a Formula SAE Car Chassis," *SAE International*, Warrendale, PA.

6. Heisler, H., 2002, *Advanced Vehicle Technology*, Butterworth-Heinemann, Woburn, MA. pp. 1

7. Perry, D.J., Azar, J.J., 1982, *Aircraft Structure*, McGraw Hill College. pp. 98, 197

8. Milliken, W.F., Milliken, D.L., 1997, *Race Car Vehicle Dynamics*, Society of Automotive Engineers.

9. Miller, C.M, 1997, *Tubing Rigidity*, http://desperadocycles.com/Lowdown_On_Tubing.html

10. Logan, D.L., 1992, *A First Course in the Finite Element Method*-2nd edition, PWS Kent, Boston.

11. Norton, R.L., 2010, Machine *Design*- 4th edition, Prentice Hall.

12. Potts, D.M., Zdravkovic, L., 1999, *Finite Element Analysis in Geotechnical Engineering: Theory*, Thomas Telford, London. pp. 74-75

13. Young, W.C., Budynas, R.G., 2002, *Roark's Formulas for Stress and Strain*, McGraw Hill, pp. 534, 735

14. Altair Engineering Inc., *Introduction to Hyperstudy.* pp. 39-84

15. Walepole, R.E., Myers, S.L., Ye, K., 2007, *Probability and Statistics for Engineers and Scientists*, Pearson Education, Inc., pp. 421-433

BIOGRAPHICAL INFORMATION

Vikram Nair, son of E. Raghavan and Pratibha Raghavan, was born on February 14, 1988, in Chennai, India. He earned his Bachelor of Science in Mechanical Engineering in May, 2009 from University of Mumbai, India.

He started his graduate studies at University of Texas at Arlington in January, 2010 and earned his Master of Science in Mechanical Engineering in May, 2012. During this time, Vikram was part of the Formula SAE racing team at UTA where he worked on frame design and also the design of an accumulator system for the Hybrid vehicle. He also worked as a Growth R&D Co-op at Medtronic Powered Surgical Solutions which involved new product design and testing of surgical equipment. His research involved the estimation of important factors which effect torsional and flexural rigidity of a space frame under the supervision of Dr. Robert Woods.